

BURIAL TAPHONOMY OF HUMAN REMAINS INTERRED IN IRON COFFINS FROM  
THE RHEM VAULT, NEW BERN, NORTH CAROLINA

by

Kate Freakley

A Signature Honors Project Presented to the

Honors College

East Carolina University

In Partial Fulfillment of the

Requirements for

Graduation with Honors

by

Kate Freakley

Greenville, NC

May 2024

Approved by:

Dr. Megan Perry

Department of Anthropology, Thomas Harriot College of Arts and Sciences

## **Abstract**

By investigating the burial taphonomy of human remains, we gain a better understanding of the important biological processes that take place following a person's death. Taphonomy is the study of how organic materials pass from the biosphere to the lithosphere through processes such as decomposition, burial, and fossilization. This investigation focused specifically on iron coffin burials, which became popular during the Civil War (1861-1865), and their effect on the preservation of human remains in above ground burials. The first part of this study consisted of examining eight subadult skeletons to create an inventory of the present bones and note the taphonomic changes that occurred. The second part of the investigation used X-Ray Fluorescence (XRF) to conduct both a qualitative and a quantitative analysis of the elemental composition of the bone surface, soft tissue, and coffin materials. This provided further insight on whether there is a positive correlation between some taphonomic changes, such as red-colored staining of the remains and iron oxidation of the iron coffins. In addition, XRF analysis was used to identify any chemical signatures of embalming, such as arsenic. Establishing results of postmortem processes will help to further understand the effects of decomposition within iron coffins, which is essential knowledge in the fields of forensics and anthropology.

## **Acknowledgements**

I would first like to thank the Rhem Family descendants, including Mr. David French, Mr. Michael Miller, and Mr. Bob and Mrs. Sandy Girton, for providing the ECU Department of Anthropology with the opportunity to excavate and study the contents of the family vault. I would also like to especially thank Dr. Megan Perry for her continuous support and guidance throughout this project, as I could not have achieved this accomplishment without her mentorship. Additional thanks to Dr. Charles Ewen for his aid in the excavation process and previous research, as well as Dr. Christopher Wolfe for serving as a faculty assessor on my thesis defense committee. Thank you as well to Ms. Bridget Cone and Ms. Jalynn Stewart, as much of their previous research paved the way for this study. I would also like to thank the members of the ECU Bioarchaeology lab, including Ms. Talia Hoffman, Ms. Delphi Huskey, and Ms. Emily Miller, for their encouragement and friendship during this process. Finally, I thank my family and friends for their love and support throughout this project and in everything that I do.

## Table of Contents

List of Tables .....	v
List of Figures .....	vi
Introduction .....	1
Background .....	1
The Rhem Family Vault .....	1
19 <sup>th</sup> Century Mortuary Practices – The Beautification of Death .....	4
The Beautification of Death and Body Preservation .....	5
Taphonomy .....	7
Taphonomy of Remains in 19 <sup>th</sup> Century Iron Coffins .....	9
X-Ray Florescence .....	12
Purpose of Study .....	14
Materials and Methods.....	15
Taphonomic Analysis .....	16
X-Ray Fluorescence Analysis .....	19
Results .....	21
Taphonomic Analysis .....	21
F.01 .....	21
F.02 .....	23
F.06 .....	26
F.07 .....	29
F.08 .....	32
F.12 .....	37
F.13 .....	39
F.19 .....	42
XRF Analysis .....	45
Discussion .....	54
Conclusion .....	57
Future Research .....	57
References .....	59

## List of Tables

Table 1: Skeletal age estimations of individuals. Age estimations are compared to reported date of death, year of death based on artifacts, and reported age at death derived from Rhem family records and coffin hardware analysis and artifacts (Joseph L. Rhem Family Bible, 1860/2020; Stewart, 2022) .....	16
Table 2: Behrensmeyer (1978) stages of bone weathering .....	18

List of Figures

Figure 1: Front aspect of the Rhem Family burial vault in Cedar Grove Cemetery, New Bern, North Carolina. Photograph taken by Dr. Megan Perry ..... 3

Figure 2: Interior damage of Rhem Family vault as seen from the front door of the vault. F.01 and F.02 are seen laying on the floor across the entrance. Photograph taken by Dr. Megan Perry..... 4

Figure 3: Human tooth development and eruption standards obtained from AlQahtani et al. (2010). The starting point is shown by the arrow. Gray indicates dentine in deciduous teeth, and green indicates that of permanent teeth..... 17

Figure 4: Individual F.01 photographed for skeletal inventory. Photograph taken by Dr. Megan Perry ..... 22

Figure 5: Coffin F.01 and contents. Note the destruction of the majority of the coffin walls. Photograph taken by Bridget Cone..... 23

Figure 6: Individual F.02 photographed for skeletal inventory. Photograph taken by Dr. Megan Perry ..... 24

Figure 7: Coffin F.02 with lid. Note the damage characterized by cracks across the center and at the foot of the coffin (left). Photograph taken by Jalyynn Stewart ..... 25

Figure 8: Coffin F.02 and contents. Photograph taken by Jalyynn Stewart ..... 25

Figure 9: Individual F.06 photographed for skeletal inventory. Photograph taken by Dr. Megan Perry ..... 27

Figure 10: Coffin F.06 and contents. Note the damage on the lower, left side of the head end of the coffin. The textile found wadded at the foot of the coffin (left) can also be seen. Photograph taken by Jalyynn Stewart ..... 28

Figure 11: Individual F.07 photographed for skeletal inventory. Photograph taken by Dr. Megan Perry ..... 30

Figure 12: Coffin F.07 and contents. Note the three-layered dress in which the individual was buried. Hair and white mold can be seen on the skull (right). Photograph taken by Jalyynn Stewart ..... 31

Figure 13: Open sock of right lower leg containing bone and soft tissue previously held inside. Photograph taken by Dr. Megan Perry ..... 31

Figure 14: Individual F.08 photographed for skeletal inventory. Photograph taken by Dr. Megan Perry .....	34
Figure 15: Coffin F.08 and contents. Note preservation of the skull (right), including hair preservation and white mold. Photograph taken by Jalynn Stewart .....	35
Figure 16: Unknown material found in coffin F.08. Photograph taken by Jalynn Stewart .....	36
Figure 17: Individual F.12 photographed for skeletal inventory. Photograph taken by Dr. Megan Perry .....	38
Figure 18: Coffin F.12 and contents. Note the preservation of textiles. Photograph taken by Bridget Cone .....	39
Figure 19: Individual F.13 skeletal remains. Remains were unable to be identified for skeletal inventory and pathological analysis. Photograph taken by Dr. Megan Perry .....	40
Figure 20a: Vertebral bodies (16) recovered from F.13. Photograph taken by Dr. Megan Perry...	41
Figure 20b: Skulls, upper limbs, and ribs of F.13. Photograph taken by Dr. Megan Perry .....	41
Figure 21: Coffin F.13 and contents. Note coloration of skull (right) and textile preservation throughout. Photograph taken by Jalynn Stewart .....	42
Figure 22: Individual F.19 photographed for skeletal inventory. Photograph taken by Dr. Megan Perry .....	44
Figure 23: Coffin F.19 and contents. Photograph taken by Jalynn Stewart .....	45
Figure 24: pXRF spectrum of the human remains from F.01. The samples tested included the pelvic ilium (F.01.1, red), lower leg and foot (F.01.2, blue), and occipital bone (F.02.3, green) .....	46
Figure 25: pXRF spectrum of F.01 human remains and coffin. The samples tested included the temporal bone (F.02.1, red), femur (F.02.2, blue), maxilla bone (F.02.3, green), scapula (F.02.4, orange), and coffin (F.02.5, black) .....	47
Figure 26: Arsenic (As) and Lead (Pb) pXRF peaks. Note how close the peaks are to each other. Image obtained from F.02 human remains pXRF spectrum .....	48
Figure 27: pXRF spectrum of F.06 human remains and coffin. The samples tested included the occipital bone (F.06.1, red), femur (F.06.2, blue), frontal bone (F.06.3, green), and coffin (F.06.4, black) .....	49
Figure 28: pXRF spectrum of F.07 human remains and coffin. The samples tested included the lower arm and soft tissue (F.07.1, red), femur (F.07.2, blue), soft tissue (F.07.3, green), and coffin (F.07.4, black) .....	50

Figure 29: pXRF spectrum of F.08 human remains. The samples tested included soft tissue (F.08.1, red), the scapula (F.08.2, blue), a portion of the ribcage and soft tissue (F.08.3, green), and an unknown material (F.08.4, orange) ..... 51

Figure 30: pXRF spectrum of F.12 human remains. The samples tested included a pelvic ilium (F.12.1, red), femur (F.12.2, blue), and the right foot and soft tissue (F.12.3, green) ..... 52

Figure 31: pXRF spectrum of F.13 human remains. The samples tested included a fibula (F.13.1, red), cranial bone (F.13.2, blue), and ilium (F.13.3, green) ..... 53

Figure 32: pXRF spectrum of F.19 human remains. The samples tested included a cranial bone (F.19.1, red), tibia (F.19.2, blue), frontal bone (F.19.3, green), and vertebrae with soft tissue (F.19.4, orange) ..... 54

## **Introduction**

The study of mortuary activity and burial practices are considered to be crucial areas of research within the fields of historical archaeology and anthropology. Each culture has a unique perception of death and the afterlife because it is a territory that is entirely unknown to the living. By studying a culture's customs and rituals, especially those surrounding the afterlife, one becomes closer to understanding that culture's beliefs, way of life, and perhaps even its cosmology. The exploration of this topic is possibly the closest anyone can come to communicating with the dead.

Another intriguing aspect of the study of the dead is the investigation of a body's decomposition. Decades of research and analysis have found consistent trends in decay and decomposition of human remains. Certain processes of decomposition are to be expected and, at this point, can even be predicted. However, due to the unique circumstantial and environmental factors of each corpse, there can be considerable variation in the timing of this process. In addition, mortuary rituals and our ancestors' treatment of the dead can impact the process of decomposition. By being aware of different practices, one can distinguish between factors that are the result of mortuary practices versus those that result from postmortem decay. Once the results of postmortem processes can be established, they can help to further understand effects of decomposition which is essential knowledge to the field of forensic anthropology.

## **Background**

### *The Rhem Family Vault*

In April of 2019, the Rhem family descendants requested that East Carolina University excavate the family's above-ground vault, in preparation for its restoration (Stewart, 2022).

Research on the Rhem family history began shortly after the request was made, and since June 2021, the East Carolina University's Bioarchaeology Lab has worked to excavate the vault as well as conduct extensive research and analysis on the artifacts and skeletal remains recovered from the vault. Such investigations helped to inventory and identify many of the individuals buried in the vault and analyze evidence for childhood health and disease, as well as to better understand the types of processes and methodologies of nineteenth and twentieth century burial practices (Cone, 2023; Stewart, 2022).

The Rhem family vault (Figure 1) is located in Cedar Grove Cemetery in the town of New Bern, North Carolina. New Bern is a riverfront city located between the Trent River and the Neuse River of North Carolina. Cedar Grove Cemetery is a park-like cemetery, established in 1800. The Rhem vault is an Egyptian-style square crypt (Hand, 2021) measuring 9.8 feet x 9.8 feet on each side with 9.5-foot-high brick walls topped by a 4-foot stepped roof, with a total height of approximately 13.5 feet (Stewart, 2022). The roof of the vault was constructed using 3.6-foot x 0.8-foot brownstone blocks, topped with a brownstone urn. The urn had fallen from the roof by the time excavation of the vault began (Stewart, 2022). The vault is partially subterranean, with a floor approximately 15 inches below ground level (Stewart, 2022). A marble plaque reading "Joseph L. Rhem's Vault" is located directly above the door. The brick structure was finished with stucco and false mortar joints (Stewart, 2022). In the interior of the vault, the north and south walls each held five 7.4-foot-long shelves, along with three movable shelves installed on the western wall (Stewart, 2022). The vault was built in the early 1850s, and used throughout 19<sup>th</sup> and 20<sup>th</sup> centuries, and clearly displays the wealth and high social status of the Rhem family at the time of its construction (Cone, 2023). When researchers arrived to excavate the vault in 2021, the interior was highly disturbed (Cone, 2023; Stewart, 2022). The

extensive damage was evident from the shelving collapse, comingled remains and artifacts scattered across the vault floor, coffins overturned and broken open, and organic growth and decay along the walls, ceiling, and floor of the vault interior (Figure 2).



Figure 1: Front aspect of the Rhem Family burial vault in Cedar Grove Cemetery, New Bern, North Carolina. Photograph taken by Dr. Megan Perry.



Figure 2: Interior damage of Rhem Family vault as seen from the front door of the vault. F.01 and F.02 are seen laying on the floor across the entrance. Photograph taken by Dr. Megan Perry.

### *19<sup>th</sup> Century Mortuary Practices – The Beautification of Death*

The Rhem vault was in use during the middle of a transitional period in U.S. mortuary rituals that began in the late eighteenth century and lasted into the nineteenth century (LeeDecker, 2009). This cultural movement, referred to as the Beautification of Death or the Cult of the Dead (LeeDecker, 2009), saw the abandonment of previous Puritan-influenced funeral practices and concepts of death amongst communities of European descent and replacement with more intricate and complex funerals. This movement increased in popularity in the middle of the 19<sup>th</sup> century, when Americans were confronted with death during the U.S. Civil War and developed a “fascination with death and dying” (Rainville, 1999: 558). With the Beautification of Death movement, funerals became more of a celebration of life and elaborate demonstrations

of respect for the dead. It was at this time that the Rural Cemetery Movement also took place, with a shift from “natural” and unlandscaped graveyards to beautified, parklike burial grounds (LeeDecker 2009; Rainville, 1999). This new burial ground format was referred to as a “cemetery,” coming from the Latin word *coemeterium*, meaning “to rest” or “to sleep,” which reflected the “peaceful sleep of death” and the promise of resurrection after death that epitomized the Beautification of Death movement (Rainville, 1999). According to LeeDecker (2009), coffins are thought to have been a display of social status but were also viewed as necessary to transport the body to the afterlife and therefore became highly important aspects of funeral services and rituals. In the early years of European settlement in the U.S., they were simply built with wood and nails, but later in the 1800s became more elaborate and ornamental (LeeDecker, 2009).

Excavation of 19<sup>th</sup> century gravesites shows clear trends in increased mortuary investment to display social status. Family tombs within cemetery grounds became more common and were seen as ornate reflections of a family’s importance and larger presence within the community (LeeDecker, 2009). In the 1860s and 1870s, following the American Civil War, intricate coffin styles and decoration reached a peak. By this time, the modern profession of undertaking had been introduced, which soon standardized not only coffins but also mortuary customs.

### *The Beautification of Death and Body Preservation*

The combination of the desire to celebrate the deceased and the need to transport bodies over long distances for burial during the Civil War led to the necessity of preserving the body for longer periods of time. In 1848 the Fisk iron coffin was patented, marking the beginning of iron

coffin popularity across the United States (Allan, 2002). Iron coffins were said to be more effective in preserving the body and protecting it from water, pests, and other environmental factors that can cause decomposition. This new style of coffin also improved the transportation of a corpse across long distances, as American soldiers killed during the Civil War were dying in places other than their hometowns.

Remains typically are kept in coffins to provide a means of protecting them from the external environment, such as destructive biota, temperature, and weather fluctuations (Pokines and Baker, 2013). However, wooden coffins that were common in the 18<sup>th</sup> century were much more vulnerable to the environment (Pokines and Baker, 2013). These coffins are more likely to break down and degrade as a result of these same environmental factors, especially when buried underground. One method for preventing coffin degradation is the construction and use of aboveground vaults, which became a common practice during the 19<sup>th</sup> century (Pokines and Baker, 2013). However, iron coffins had a greater ability to withstand external environmental factors, hindering decomposition of the body for a much longer period of time than the standard wooden coffin (Allan, 2002; Pokines and Baker, 2013). The interior of iron coffins has anaerobic environmental conditions which permits extended preservation of any organic materials they may contain (Pokines and Baker, 2013).

In addition to changes in coffin materials to help preserve bodies for longer periods of mourning, embalming became a common practice to lengthen the interval between death and advanced decomposition, as well as to prevent the spread of infection before and after burial (Allen, 2002; Brenner, 2014; Geddes, 1981). The art and science of embalming can be traced back to ancient Egyptian culture where it was believed that preserving a corpse via mummification would allow for the soul to return to its body after death (Ezugworie et al.,

2008). In late 16<sup>th</sup> and early 17<sup>th</sup> century Western Europe and the British colonies, embalming was reserved for individuals of high social status such as royalty or high-ranking members of the church, whose funerals were usually delayed for more public ceremonies (Miller et al., 2004). Methodological records of this time period show that the organs of the abdomen, chest, and head were each removed, and those areas cleaned and then filled with a powder or balm made up of numerous ingredients that likely varied depending on the region and embalmer (Ezugworie et al., 2008; Miller et al., 2004). Miller et al. (2004) states that dry salt, “Allum of glasse...Balme hearb, or hoarie Mints, Wormwood, water mints, Sage, Rosemary, Organum, Calamint,” and, “Time,” among other substances were ground together and used to fill the cavities where organs were removed. This traditional practice of embalming persisted in the U.S. until the early 19<sup>th</sup> century, and only then was it used sparingly. The American Civil War marks the development of what is considered modern day embalming in which all blood and gases are removed from the body and a disinfecting fluid is inserted. By the late 19<sup>th</sup> and early 20<sup>th</sup> centuries, embalming fluid was primarily arsenic or alumina salts which were later replaced by formaldehyde (Brenner, 2014; Ezugworie et al., 2008). Occasionally, evidence of embalming has been found in archaeological explorations of 19<sup>th</sup> century burials, as discussed below.

### *Taphonomy*

Understanding burial practices must include an investigation of taphonomy of the human remains in order to distinguish between human behaviors (such as mortuary practices) and natural factors that have affected the skeleton. Taphonomy is the study of fossilization and focuses on the decomposition processes a body undergoes from the time of death to the point of recovery. Its broad definition takes on a multidisciplinary approach encompassing biological,

cultural, and geological analyses (Sorg and Haglund, 1996). Within forensic anthropology, taphonomic analysis is commonly used in understanding paleoenvironments, identifying factors that cause decomposition of human bone, and differentiating human from nonhuman causes of bone modification. Additionally, forensic anthropologists are interested in taphonomic processes of soft tissue, such as rates of decomposition, trends of decomposition, disarticulation, and dispersion of remains (Sorg and Haglund, 1996). Normal decomposition processes of human remains includes autolysis, fermentation, decay, petrification, and saponification which occur in aerobic burial environments and are affected by water infiltration and soil composition (Owsley and Compton, 1997). The decomposition process of human remains can generally be divided into five stages: fresh, bloat, active decay, advanced decay, and dry remains or skeletonization (Iqbal et al., 2018). The conversion of soft tissue to a “leather-like” consistency over the bone occurs during the final stage of decomposition, and skeletonization, which occurs later in this stage, is identified by over 50% of the body being exposed bones (Iqbal et al., 2018). The skeletonization stage continues until the point at which only resistant bones, teeth, and cartilage are left. Following this stage, the processes of chemical weathering and diagenesis occur over a longer period of time, affecting the organic and inorganic composition of the remains (Iqbal et al., 2018).

Skeletonized bone is subject to weathering which typically leads to swift alteration in the appearance of the bone (Behrensmeyer, 1978). Behrensmeyer (1978) defines weathering as the process of the original organic and inorganic make-up of a bone are separated and destroyed by physical and chemical agents, and she provides evidence that the stages of bone weathering are predictably linked to the time since death of an individual. These five stages range from the bone surface having no signs of weathering (Stage 0) to the bone falling apart *in situ* and

exposure of cancellous bone (Stage 5) (Behrensmeyer, 1978). When examining stages of decomposition and weathering, a pathological analysis can be conducted in order to reveal any diseases an individual may have had that would have affected the bone condition (Buikstra and Ubelaker, 1994).

Biotic factors (e.g., temperature, local biome, and scavenger activity), geological factors (e.g., burial environment and soil conditions), and anthropogenic factors (e.g., ante-mortem or post-mortem injuries, absence or presence of clothing or wrappings, and burial type) can each have an impact on decomposition (Iqbal et al., 2018). Analyzing the decomposition trends provides for better understanding of the environment and circumstances in which an individual's remains were left and how they have been affected over time.

#### *Taphonomy of Remains in 19<sup>th</sup> Century Iron Coffins*

Metal coffins that were in use during the 19<sup>th</sup> century altered the normal decomposition process of human remains. Although little evidence of the manufacturing process of iron coffins or catalogues produced by Fisk, Crane and Breed, and other 19<sup>th</sup> century producers of iron coffins exist today, some iron coffins have been found during archaeological excavations. The preservation of the human remains, textiles, and leather within the iron coffins varies widely, from excellent preservation of bones and soft tissue as well as textiles (Owsley and Compton, 1997), to remains having good preservation, dark coloration, and being fully clothed (Owsley, 2006), to fair skeletal preservation, dark orange coloration, and little to no clothing preservation (Bricker et al., 2013). Additionally, Bricker et al. (2013) notes the demineralization of bone and acceleration of deterioration caused by clothing preservation and water infiltration. Clothing preservation varied depending on the types of material from which the cloth was made when

exposed to water. Parts of the upper body and skull were well preserved, but the more fragile parts of the axial skeleton and the lower body were completely deteriorated (Bricker et al., 2013). Another taphonomic study examined different levels of textile preservation in human burials and found that most cases of well-preserved textiles resulted in mummified or slightly mummified remains. Very few cases of mostly decayed textiles contained mummified human remains (Lipkin, 2021). Owsley and Compton (1997) discuss one case of an individual whose preservation indicated that time elapsed since death had been approximately one year, but once the body had been identified, historical records confirmed that the man had actually been interred 113 years before the discovery of his coffin. The intact, sealed iron coffin usually slows the overall decomposition rate of human remains and textiles and leads to these varied preservation states, but once the coffin interior is exposed to the natural environment, often from the breaching of the viewing window, the typical, more predictable decomposition processes begin (Pokines and Baker, 2013).

In addition, interaction between natural decomposition of the bodies, embalming chemicals, and the coffin materials was found to alter the appearance of the human remains. In four coffins dating to the 1850s from southeastern Virginia, the amalgamation of natural substances produced from the bodies' decomposition with lead sulfates found in the paint coating the inside of the coffins resulted in the accumulation of iron sulfides within the coffins (Bricker et al., 2013). In addition, interaction between certain metals used in coffin manufacturing, such as iron, copper and mercury, and the human remains, can result in red, green, or dark brown staining of the bones and soft tissues (Dupras and Schultz, 2014; Pokines et al., 2009; Pokines et al., 2016; Schultz et al., 2003). This will be distinguished from discoloration due to heat exposure, which can cause bone to become brown or black, or it can even turn white to blue-gray

at extremely high temperatures (i.e. 800 degrees centigrade), and biotic factors, such as bacteria, plants, and natural minerals that typically cause bone to be colored tan, red-brown, grey, or almost black (Buikstra & Ubelaker, 1994). Some of this staining may also be connected to the effects of embalming as well as decomposition (Pokines et al. 2016).

An exceptional example of embalming effects was the presence of a crystal-like substance concentrated in the head, chest, and abdomen of Philip Calvert, who was buried in a lead coffin in the 17<sup>th</sup> century. Neutron Activation Analysis (NAA) of the material found high concentrations of calcium, sodium, chlorine, aluminum, copper, and magnesium (Miller et al., 2004). Presence of these substances, especially that of the sodium and aluminum, is likely directly linked to the embalming, and the prominent development of the crystalline material was likely due to the interaction between these elements and the metals in the coffin.

The human remains and associated materials from the Rhem iron coffins also display staining and the possible result of chemical reaction between the coffin materials and body decomposition and, possibly, embalming chemicals. To understand the unique taphonomic environments of these coffins and how they impacted human decomposition, this project utilizes both general taphonomic analysis and study of the elemental composition of the coffins and the remains through X-Ray Fluorescence (XRF). Knowing the overall decomposition state of the bodies as well as the composition of the unknown staining should reveal the likely chemical reaction that occurred within the various coffin environments. In this case, the goal of conducting a taphonomic analysis is to determine postmortem changes and decomposition states of each individual interred in a metallic coffin.

## *X-Ray Florescence*

Since their discovery by Wilhelm Conrad Röntgen in 1895, X-rays have been a powerful tool across nearly all scientific fields, most notably in the field of medicine (Beckhoff et al., 2007; Berkowitz, 2006). In 1913, Henry Moseley experimented with x-ray technology and developed Moseley's Law which relates the frequency of elemental x-ray emissions to the element's atomic number (Berkowitz, 2006). This is the concept upon which X-Ray Fluorescence (XRF) technology is based. Eventually, as research continued and the value of X-ray technology was further realized, the XRF spectrometer was invented by Abbott in 1948. XRF is a tool that allows for the identification of materials by presenting a qualitative and quantitative elemental composition of an object. Thus, in addition to fields such as materials science, XRF has become a valuable addition to the study of artifacts and historical objects in archaeology, art history, and cultural heritage. The development of portable XRF (pXRF) and hand-held XRF (HH-XRF) technologies has resulted in even wider use in archaeology (Beckhoff et al., 2007; Fernandes et al., 2013). XRF analysis of tools, ceramics, and other artifacts, provides a better understanding of the state or make-up of these objects to help explain ancient technologies as well as approaches to conservation of them. For example, Fernandes and colleagues used HH-XRF to analyze recovered copper-alloyed artifacts of Roman origin. Along with determining the artifacts' compositions and the effects of corrosion, the researchers were able to establish evidence in support of the application of XRF analysis to archaeological investigations. While other methods such as Neutron Activation Analysis (NAA) (Miller et al., 2004), laser mass spectrometry, Ion Beam Analysis (IBA), Scanning Electron Microscope Energy Dispersive X-Ray Spectroscopy (SEM-EDS) (Andrade et al., 2014), and infrared technology (Henderson, 2015) can be used to identify the elemental composition of objects, XRF

is preferred due to its straightforward procedure, ease of sample preparation, and overall greater accuracy (Adan-Bayewitz et al., 2007). Portable XRF (pXRF), specifically, is highly advantageous for field studies in anthropology, archaeology, geology, and art, as it provides a user-friendly, non-destructive technique (Gomes et al., 2024). The use of pXRF is beneficial for the analysis of human remains, where invasive sample extraction is not usually possible (Mann et al., 2021; Gomes et al., 2024; Santos, 2020), because sample powdering is not necessary (Gomes et al., 2024; Zhou et al., 2022). Conrey et al. (2014) uses pXRF spectrometry to examine archeological samples in response to its growing use within archaeological fields.

The application of pXRF to the analysis of human skeletal remains is less advanced than the study of artifacts, but its utilization is continuing to expand. Most studies have focused on using pXRF to individuate commingled remains, which assumes that humans have bone chemistry unique enough to sort them by individual (McGarry et al., (2021) Perrone et al., 2014). Nganvongpanit et al. (2016) and Zimmerman et al. (2015) also use pXRF to distinguish human remains from non-human remains. XRF also can be used to understand how particular elements, such as strontium, positively or negatively affect childhood bone development (Specht et al., 2017), or quantify the levels of toxic metals in bone such as lead (Specht et al., 2014, 2019). Other studies have used XRF to identify if bone pathological lesions such as cribra cranii (Gomes et al., 2021), cribra orbitalia (Çirak, 2016; Kilburn et al., 2021) both of which are associated with anemia, syphilis (Ioannou et al., 2017; Kilburn et al., 2021), osteosclerotic dysplasia (Magalhães et al., 2021), osteoporosis (Zdral et al., 2021), rickets, scurvy, and diffuse idiopathic skeletal hyperostosis (DISH) (Kilburn et al., 2021), which are all conditions that result in altered bone chemistry. Portable XRF has also been used to identify chemical treatments of disease, such as mercury used to treat syphilis in post-medieval London (Zuckerman, 2016), and the chemicals

used for mummification in ancient Egypt. Portable XRF has also been used to characterize the chemical alteration of bone due to taphonomic processes to identify those that have undergone significant diagenesis (Granite 2012; Lopez-Costas et al. 2016). These researchers chose to use pXRF over the other methods because of its portability, quick measurement time, and simple use. In summary, X-ray fluorescent analysis is a scientific technique which can be used to investigate the elemental make-up of materials, including human bone, in a precise and non-destructive manner.

### *Purpose of Study*

This research was conducted to determine the taphonomic effects of burial in a Fisk-style cast iron coffin on human remains, including identifying the elemental composition of metallic staining on the bone surface, and understand the decomposition processes within the coffins, including testing for evidence of embalming chemicals. To accomplish this, a complete taphonomic study of the skeletal remains excavated from eight of the eleven iron coffins from the Rhem vault was conducted. This revealed any macroscopically visible chemical or physical modifications to the corpse that may have occurred postmortem, including levels of preservation. Then, the elemental composition of the human remains and the coffins was obtained using pXRF not only to identify the sources of bone staining and discoloration but also to identify chemicals that could have been used for embalming.

It was hypothesized that overall preservation of an individual would reflect the state of the coffin from which they were recovered. In general, better-preserved bodies, characterized by good bone composition and soft tissue preservation, would be recovered from coffins which had not been damaged or opened before excavation. Coffins that had been damaged were expected

to contain poorly preserved remains comprised of incomplete or missing bones that are friable or fragile as well as no soft tissue preservation. Textile preservation should follow similar trends, providing further insight to the overall effect of the coffin environment. Additionally, clothing was expected to have a role in the preservation of remains; those covered or wrapped in clothing were expected to be uniquely preserved and potentially mummified more so than those that are not, as seen in Lipkin (2021).

XRF analysis was expected to reveal similar trends between the elemental composition of an individual's remains and that of the coffin in which they were buried. In other words, the elements found in the coffin materials, specifically iron and lead, were expected to also be present on or within the bone and soft tissue remains. Furthermore, it was hypothesized that the remains found in coffins that were intact would have a higher intensity of iron, lead, and other metals from the coffin material. Lastly, the presence and quantity of metallic staining was expected to be directly correlated to the condition of the coffin; the better condition in which the coffin was found, the more metallic staining would be observed (Bricker et al., 2013).

This procedure was conducted so that a better understanding of both nineteenth century mortuary behaviors, particularly related to embalming or other body preparation practices, as well as chemical decomposition processes could be obtained.

## **Materials and Methods**

A total of fourteen metal coffins, each containing the remains of individual Rhem family members, were recovered from the family vault. Ten of the coffins, all containing children, were examples of Fisk-type iron coffins, and another (F.01) was made from different metallic materials. Eight of the coffins (seven of the Fisk-type iron coffins, one of an unknown metal)

were included in this research (Table 1). Three of the coffins in this study (F.12, F.13, F.19) held remains that were able to be identified, using records of Rhem Family history and in some cases, coffin plates engraved with the decedent’s name. The other five remain unidentified. Because these coffins only contained children who had not reached skeletal maturity, their sex and stature could not be assessed. However, age estimations can be made using dental formation (AlQahtani et al., 2010) as well as bone measurements (Cardoso et al., 2014; Cardoso et al., 2017). An inventory of personal items and clothing found in each coffin was also collected in a previous study (Stewart, 2022).

COFFIN NUMBER	NAME	REPORTED DATE OF DEATH	YEAR OF DEATH BASED ON ARTIFACTS	REPORTED AGE AT DEATH	SKELETAL AGE AT DEATH
F.01	Unknown		1870s-1880s		4-8 months
F.02	Unknown		1870s		5-6 years
F.06	Unknown		Before 1870		5-9 months
F.07	Unknown		1870s		4.5-9.5 months
F.08	Unknown		1870s		7-9 years
F.12	Lula Newbernia Rhem	1867	1860s	5 years	4.5-6.5 years
F.13	Mary B. Rhem	1861	1860s	1 year	Subadult
F.19	Hugh Dudley Rhem	1873	1870s	1 year	Birth +/- 2 weeks

Table 1: Skeletal age estimations of individuals. Age estimations are compared to reported date of death, year of death based on artifacts, and reported age at death derived from Rhem family records and coffin hardware analysis and artifacts (Joseph L. Rhem Family Bible, 1860/2020; Stewart, 2022).

### *Taphonomic Analysis*

The first part of data collection began with a taphonomic and pathological investigation of the recovered remains. The skeletons had been removed from the coffins and the remains cleaned prior to this analysis. Each individual was laid out anatomically and photographed, and an inventory of skeletal elements was added to a FileMaker Pro v. 20 database. Any remaining clothing or textiles attached to the body were removed, but soft tissue was left in place.

Additional photographs were taken of any significant features. This included well preserved soft

tissue, bone pathologies and morphologies, and clothing that could not be easily removed from the body. Ages of the children were estimated using dental formation following AlQahtani et al. (2010) (Figure 3), long bone and shoulder and pelvic girdle measurements using Cardoso et al. (2014, 2017), and fusion of primary and secondary ossification centers based on Scheuer and Black (2010). In addition to age estimation, evidence of pathological lesions and general preservation of the bodies was recorded.

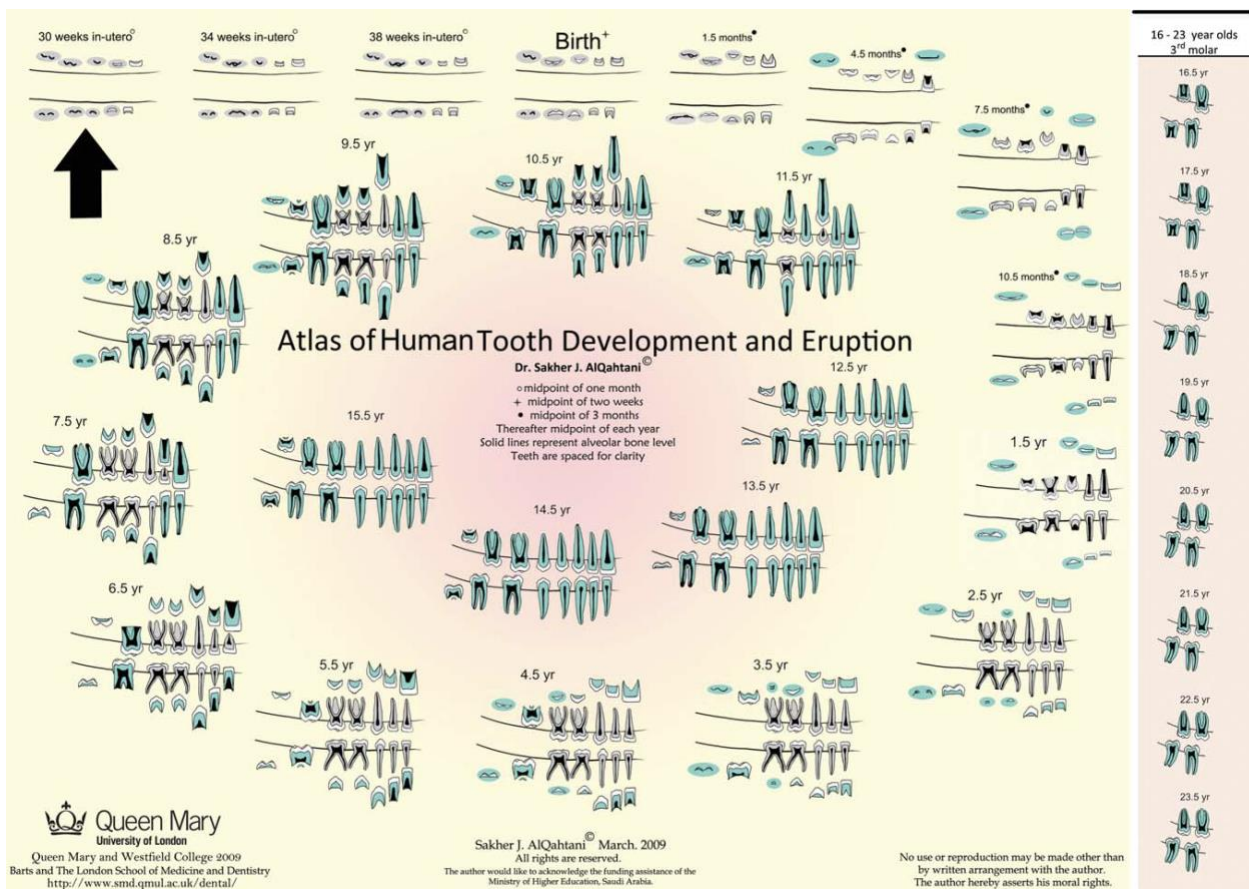


Figure 3: Human tooth development and eruption standards obtained from AlQahtani et al. (2010). The starting point is shown by the arrow. Gray indicates dentine in deciduous teeth, and green indicates that of permanent teeth.

Taphonomic data collection followed *Standard for Data Collection from Human Skeletal Remains* (Buikstra and Ubelaker, 1994). Bone staining was recorded by color and location on

the bone. Changes in the surface texture of the bones, such as weathering, were also noted. Stages of weathering were reported based on Behrensmeyer's standards (Table 2; Behrensmeyer, 1978). Finally, alterations in bone shape were noted. Temperatures high enough to induce calcination can cause bone to warp and/or shrink. Dehydration, salt accumulation, and heat can break or fragment bones. Additionally, because it was known that the remains had been exposed to water while interred in the family vault (Stewart, 2022), they were examined for weathering specifically due to water damage. This is indicated by cortical exfoliation on all bones and longitudinal cracking on long bones (Murphy et al., 1981; Pokines et al., 2018).

WEATHERING STAGE	CHARACTERISTICS
STAGE 0	Bone surface shows no sign of cracking or flaking due to weathering. Usually bone is still greasy, marrow cavities contain tissue, skin and muscle/ligament may cover part or all of the bone surface.
STAGE 1	Bone shows cracking, normally parallel to the fiber structure (e.g., longitudinal in long bones). Articular surfaces may show mosaic cracking of covering tissue as well as the bone itself. Fat, skin, and other tissue may or may not be present.
STAGE 2	Outermost concentric thin layers of bone show flaking, usually associated with cracks, in that the bone edges along the cracks tend to separate and flake first. Long thin flacks, with one or more sides still attached to the bone, are common in the initial part of Stage 2. Deeper and more extensive flaking follows, until most of the outermost bone is gone. Crack edges are usually angular in cross-section. Remnants of ligaments, cartilage, and skin may be present.
STAGE 3	Bone surface is characterized by patches of rough, homogeneously weathered compact bone, resulting in a fibrous texture. In these patches, all the external, concentrically layered bone has been removed. Gradually, the patches extend to cover the entire bone surface. Weathering does not penetrate deeper than 1.0-1.5 mm at this stage, and bone fibers are still firmly attached to each other. Crack edges usually are rounded in cross-section. Tissue rarely present at this stage.

STAGE 4	The bone surface is coarsely fibrous and rough in texture; large and small splinters occur and may be loose enough to fall away from the bone when it is moved. Weathering penetrates inner cavities. Cracks are open and have splintered or rounded edges.
STAGE 5	Bone is falling apart <i>in situ</i> , with large splinters lying around what remains of the whole, which is fragile and easily broken by moving. Original bone shape may be difficult to determine. Cancellous bone usually exposed, when present, and may outlast all traces of the former more compact, outer parts of the bones.

Table 2: Behrensmeyer (1978) stages of bone weathering.

### *X-Ray Fluorescence Analysis*

During the second part of data collection, pXRF analysis was used to examine the cause of the unusual rust-like staining observed on the skeletal remains and metallic globules found within some of the coffin environments. Three to four skeletal elements of differing preservation and amount of staining were irradiated along with the internal and external surfaces of three coffins. The elemental composition of the human remains and the coffins were tested using a Tracer 5 handheld XRF that can detect fluorine through uranium. The pXRF contains a 1 µm graphene window silicon drift detector and a 50kV (4W) rhodium end-window tube. The pXRF was run in spectrometer mode using an 8 mm collimator under two different filter settings. The human remains elements were measured with the 75 µm Cu; 25 µm Ti; 200 µm Al (3-violet) filter at 50KeV and current starting at 20 µA for 60 seconds. This setting is best for excitation of mercury (Hg), lead (Pb), and arsenic (As) that may have been used for embalming or medical treatment.

Additionally, pXRF analysis was conducted on the external surface, internal surface, and seal of three of the metal coffins: F.02, F.06, and F.07. External rust and other adherents were removed from the coffin metal using a grinding attachment on a Dremel rotary device. The metal coffin data was collected using the 25 µm Ti; 300 µm Al (1-yellow) filter with the voltage

set at 50keV and current starting at 35  $\mu$ A for 60 seconds. These results were compared to the human remains to link the residue and staining on and around the remains to degradation of the coffins. The spectra were examined for the presence of elements not generally found in human remains or identified in the coffin scans for evidence of additional treatment of the remains after death.

When examining the bone samples, it was expected that high levels of calcium (Ca) and phosphorous (P), would be detected because bone is naturally made of these minerals (Woodard, 1962; Carvalho et al., 2004; Pemmer et al., 2013) Carbon (C), nitrogen (N), hydrogen (H), and oxygen (O) are also found in bone, but are too light to be detected by the pXRF. Additionally, silicon (Si), potassium (K), zinc (Zn), and strontium (Sr) were also expected as they are commonly taken up during an individual's lifetime and found within bone at lower levels (Blumenthal, 1990; Carvalho et al., 2004; Pemmer et al., 2013;). The coffins were expected to be primarily made up of iron (Fe) and sealed by lead (Pb), as this was the common design of metallic coffins during this time (Allan, 2002). Additionally, it was anticipated that coffin XRF analysis may contain additional traces of lead, zinc, copper (Cu), nickel (Ni), and tin (Ti) from coffin hardware (e.g., handles, screws, etc.). Finally, pXRF spectra were analyzed for arsenic (As), and elements that make up zinc chloride ( $ZnCl_2$ ), copper sulfate ( $CuSO_4$ ), potassium carbonate ( $K_2CO_3$ ), aluminum sulfate ( $Al_3(SO_4)_3$ ), bichloride of mercury ( $HgCl_2$ ), and turpentine oils ( $C_{10}H_{16}$ ) as these chemicals were commonly used for embalming fluids during the 19<sup>th</sup> century (Brenner, 2014). Unfortunately, formaldehyde ( $CH_2O$ ), which was more commonly used for embalming in the 20<sup>th</sup> century (Brenner, 2014), cannot be detected by the pXRF.

## **Results**

### *Taphonomic Analysis*

#### F.01

Individual F.01 was found in a hexagonal iron coffin in two pieces. The coffin was lying north to south just within the entrance of the vault and the south wall. The estimated burial date was 1870-1880s based on coffin hardware (Stewart, 2022). The individual was wrapped in a blanket and cloth diaper (Stewart, 2022). In terms of preservation, much of the ribs and the arms were not present. The lower body was lighter in color compared to the upper body. The overall coloration of the remains gets gradually darker as you move up the body. No metallic staining or rust-like coloration was observed. The femora, pelvis, and sacrum were encased in mummified tissue covered with woven cloth which was removed for analysis of the skeleton. The tibiae, fibulae, and feet are articulated and covered with mummified soft tissue. No soft tissue was found in the upper body.

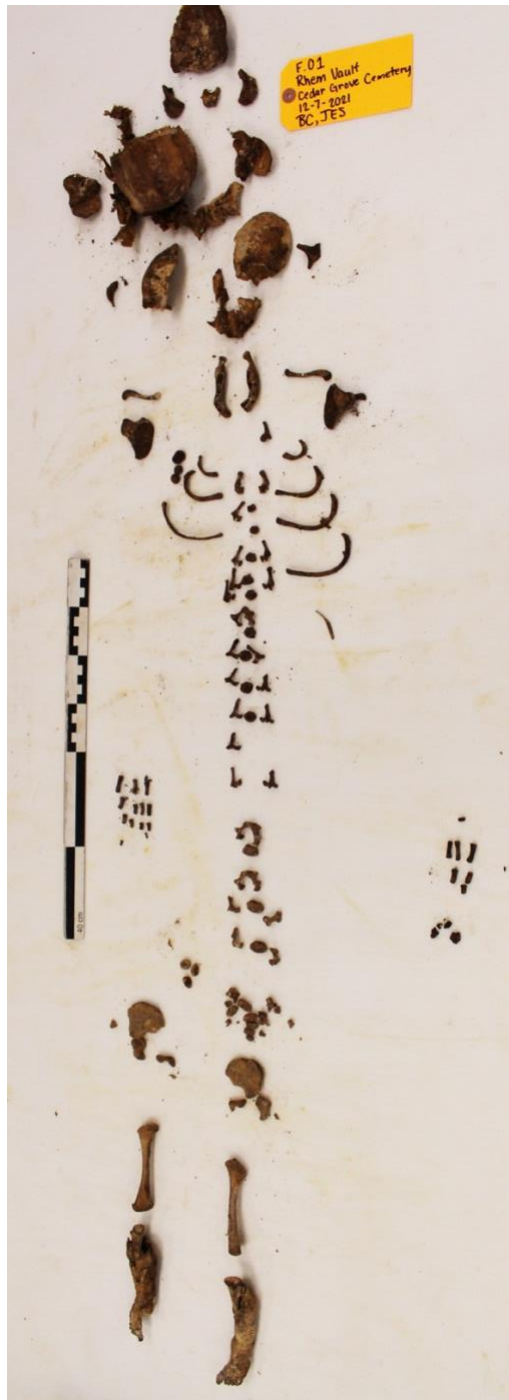


Figure 4: Individual F.01 photographed for skeletal inventory. Photograph taken by Dr. Megan Perry.



Figure 5: Coffin F.01 and contents. Note the destruction of the majority of the coffin walls. Photograph taken by Bridget Cone.

Several of the bones that belonged to individual F.01 were found intact. The scapulae, clavicles, pelvic girdle, lower limbs, sacral vertebrae, and the majority of the skull bones were complete. Scurvy was identified based on porosity of bone in the basilar portion of occipital, sphenoid, scapulae, and orbitals. Additionally, femoral anteversion was observed, causing the individual's knees to be pointed inward suggesting that he/she was likely pigeon toed. F.01 was estimated to be 4.5 months old  $\pm$  3 months based on dental formation.

## F.02

Individual F.02 was discovered in a curved lancelet coffin lying upside down within the door of the vault. The proposed burial date based on coffin hardware was indeterminate (Stewart et al., 2022). Observations of the overall preservation revealed that the distal and proximal ends of most long bones were broken or missing. Additionally, the left side was better preserved than the right. The skull was complete but in pieces because this was a subadult individual whose

cranial bones had not yet fused. Some white mold could be seen on parts of the skull, but no hair was noted.



Figure 6: Individual F.02 photographed for skeletal inventory. Photograph taken by Dr. Megan Perry.



Figure 7: Coffin F.02 with lid. Note the damage characterized by cracks across the center and at the foot of the coffin (left).  
Photograph taken by Jalynn Stewart.



Figure 8: Coffin F.02 and contents. Photograph taken by Jalynn Stewart.

The lower limbs showed more overall signs of weathering which appeared to be from water exposure, indicated by the exposure of cortical bone throughout the majority of the

skeleton (Murphy et al., 1981; Pokines et al., 2018). The right side of the body was more weathered than the left, and much of the cortical bone had been worn off, revealing inner bone. F.02 was estimated to be 5.5 years old  $\pm$  0.5 years according to stages of subadult dental formation. This fit with the stage of fusion of the vertebral ossification centers of the vertebrae which was estimated as 4-6 years.

#### F.06

Individual F.06 was recovered from a torpedo-shaped iron coffin located on the north shelves of the vault. The proposed burial date was sometime before 1870 based on the tapered edges and shape of the coffin (Stewart, 2022). A textile was found wadded at the foot of the coffin, and a coffin lining and fringe were recovered (Stewart, 2022). The lower, left side of the head end of the coffin had been cracked and corroded, leaving a hole in that area. No clothing had been preserved within the coffin. The majority of bones present were incomplete. No carpals, metacarpals, tarsals, metatarsals, or phalanges were recovered. The recovered skull bones consisted of mainly fragments. Preservation of the remains was overall poor, especially across the appendicular skeleton.



Figure 9: Individual F.06 photographed for skeletal inventory. Photograph taken by Dr. Megan Perry.



Figure 10: Coffin F.06 and contents. Note the damage on the lower, left side of the head end of the coffin. The textile found wadded at the foot of the coffin (left) can also be seen. Photograph taken by Jalynn Stewart.

Much of the cortical bone surface and metaphyses had been affected by erosion and taphonomic change. The internal and external surfaces of the left cranium were covered in a white powdery substance, likely mold. The entire surface of the mandible exhibited stage 1 weathering, indicated by cracking and cortical erosion. The left arm was friable and showed cracking across the surface. Examination of the distal ends of the right humerus and left and right femora revealed metaphyseal plate erosion and distinct layering of cortical bone and spongy bone of the plate surface. Little soft tissue was preserved and was only present around the proximal and distal ends of the right femur and proximal end of the right tibia. F.06 was

estimated to be 7.5 months old  $\pm$  3 months. This estimation was made based on dental formation standards.

#### F.07

Individual F.07 was found in a torpedo-shaped iron coffin located on the north shelves of the family vault. The coffin was completely closed and intact when excavation occurred (Stewart, 2022), and inside the coffin (Figure 12), a three-layered dress, cloth diaper, boots, and socks were all fully intact (Stewart, 2022). A noticeable red tint was noted throughout much of the bone and soft tissue. Thoracic vertebrae 1-9 (T1-T9) were all present and were encased in soft tissue. The right humerus, right and left temporals, right hand, radius, and ulna, left hand, left and right parietals, left and right maxillae, right femur, left foot, tibia and fibula, and right foot were all covered by soft tissue. Some ribs and parts of the ilia were also covered by localized soft tissue. Additionally, the right hand, radius, and ulna, left hand, right foot, and left foot, tibia, and fibula were articulated due to soft tissue preservation. Some hair was still present on the skull, and white mold had grown on many of the skull fragments.



Figure 11: Individual F.07 photographed for skeletal inventory. Photograph taken by Dr. Megan Perry.



Figure 12: Coffin F.07 and contents. Note the three-layered dress in which the individual was buried. Hair and white mold can be seen on the skull (right). Photograph taken by Jalyann Stewart.



Figure 13: Open sock of right lower leg containing bone and soft tissue previously held inside. Photograph taken by Dr. Megan Perry.

In this case, the preserved soft tissue had a clay-like consistency. It was partly mummified but moist and flexible. Socks that were covering the lower legs and feet were removed, and these areas of the body were still covered in soft, moist soft tissue (Figure 13). No noticeable flaking or other signs of weathering of the bones was observed.

During the pathological analysis, porosity on the greater wing of the sphenoid was observed. This is an indication of scurvy, indicating a lack of vitamin C likely due to the individual's diet. No other signs of scurvy were identified. Many bones were covered with periosteum, making it difficult to observe the cortical surface for pathological analysis. This included the left and right scapulae, left and right clavicles, left radius and ulna, pelvic bones, left femur, right fibula and tibia, and many of the left and right ribs. F.07 was estimated to be 7.5 months old  $\pm$  3 months based on stages of dental formation and bone metrics.

#### F.08

Individual F.08 was found in a curved lancelet iron coffin located on the north shelves of the vault (Stewart, 2022). Textile buttons and boots with laces and scalloped edging were recovered from the coffin which was lined with pine straw (Stewart, 2022). Additionally, many pieces of an unknown material were found throughout this coffin (Figure 16). The pieces were small and irregular in shape, and they were all black and shiny or metallic in color. This unknown material was not found in any other coffins, and samples were collected for pXRF analysis. While most of the skeleton was present, it was in an overall poorly preserved state, with the ulnae in particular in poor condition. Tough, dry, and somewhat friable soft tissue was adhered to many elements, keeping bones articulated in some cases. The majority of soft tissue was located around the spine and ribs. The thorax consisted of three main sections or chunks:

Cervical vertebra 7 to thoracic vertebra 3 (C7-T3), thoracic vertebra 4 to lumbar vertebra 2 (T4-L2), and right ribs 1 or 2 to ribs 7 or 8. Rib heads were embedded in these sections and could not easily be inventoried. The vertebrae also could not be removed from the surrounding matrix.

The cranium was almost fully intact, and soft tissue was present primarily on the left frontal, left and right maxillae, left and right parietals, and part of the left and right temporals. Hair was also present on the cranium, and some mold found on the inside of the upper cranium. Additionally, soft tissue was also preserved on the proximal left humerus, distal left radius, parts of the shaft of the left and right femora and tibiae, and left and right tarsals. The right tarsals, metatarsals, and phalanges were articulated with soft tissue inside a sock, which was removed for examination.



Figure 14: Individual F.08 photographed for skeletal inventory. Photograph taken by Dr. Megan Perry.



Figure 15: Coffin F.08 and contents. Note preservation of the skull (right), including hair preservation and white mold. Photograph taken by Jalynn Stewart.



Figure 16: Unknown material found in coffin F.08. Photograph taken by Jalynn Stewart.

Many signs of stage 2 weathering were observed throughout the remains. Flaking was especially noticeable on long bones. The radii apparently were warped, likely due to water infiltration into the coffin rather than an in vivo process. Metallic staining was not very present except around thoracic vertebrae and some of the upper ribs, mainly in the three sections of the thorax. F.08 was estimated to be 7.5 years old  $\pm$  1 year, as determined by dental formation and bone metrics.

## F.12

Individual F.12 was recovered in a torpedo-shaped iron coffin located on the south shelves of the vault. Based on the style of clothing in which the individual was buried, the proposed burial date is the 1860s (Stewart, 2022), and the individual was discovered to be the probable identity Lula Newbernia Rhem (1862-1867) (Stewart, 2022). An intact dress, petticoat, stockings, boots, coffin lining, and head cushion with lace were all recovered from the coffin (Stewart, 2022). Dry, brittle, potentially mummified tissue covered much of the bone, obscuring the cortical surface. The nature of this tissue appeared differently on the radii and ulnae versus the hands and fingers, as well as on those areas versus the lower limbs. The soft tissue on the radii and ulnae in particular seemed to be almost like an involucrum, and it was not entirely clear that it wasn't bone. However, the cortical bone, though poorly preserved, could be seen underneath. The mandible contained a large amount of this material adhering to its surface, while the skull had hardly any. The top half of the body was dark in color, almost looking charred, and the bottom half appeared much lighter. No rusted coloration was observed.

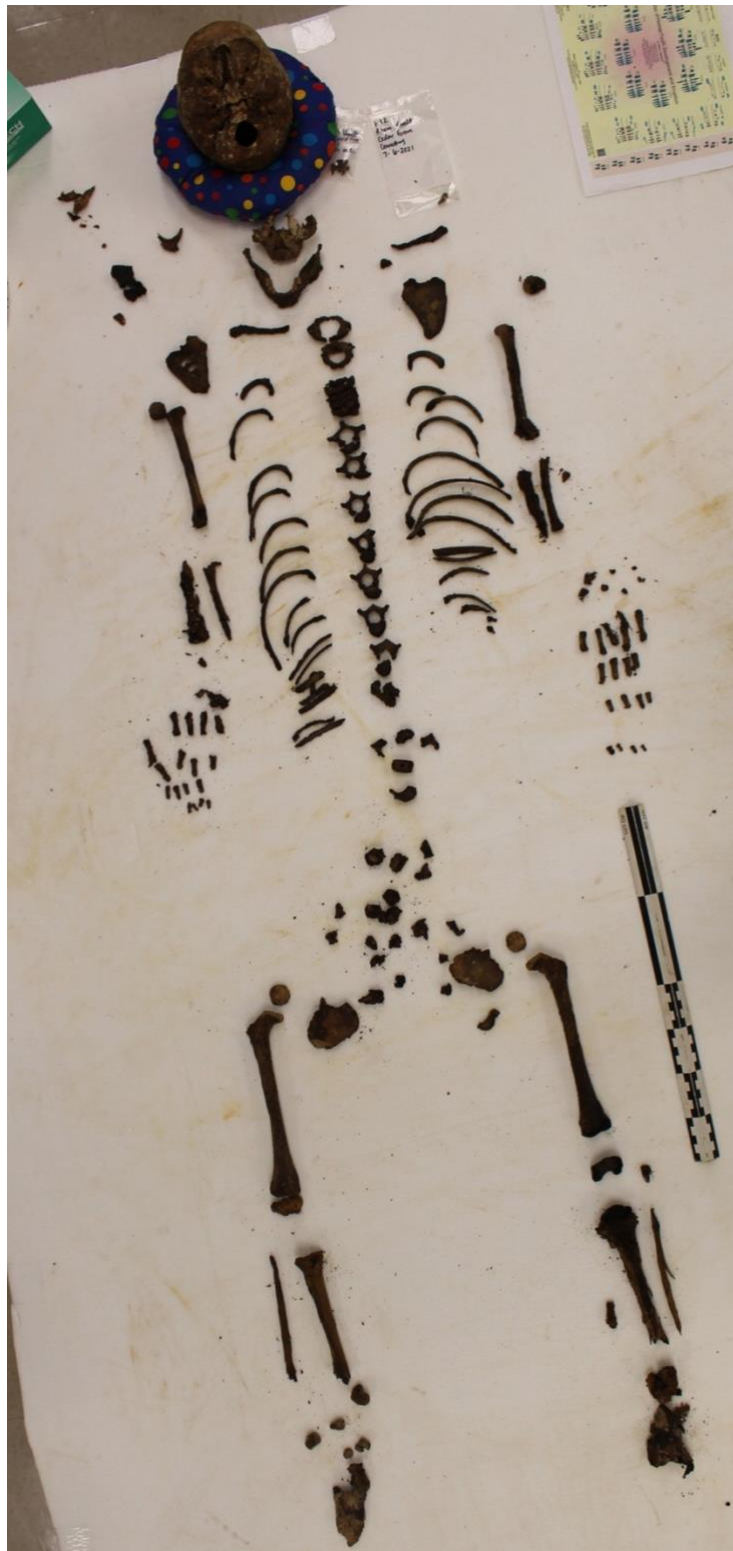


Figure 17: Individual F.12 photographed for skeletal inventory. Photograph taken by Dr. Megan Perry.



Figure 18: Coffin F.12 and contents. Note the preservation of textiles. Photograph taken by Bridget Cone.

The metatarsals and phalanges of both feet were articulated by soft tissue, making it difficult to identify which tarsals were present or missing. The distal arm and distal leg seemed to be the areas of poorest preservation, along with the thoracic and lumbar vertebrae and the sacrum which were also poorly preserved. F.12 was estimated to be 5.5 years old  $\pm$  1 year based on dental formation, epiphyseal union, and bone metrics.

### F.13

Individual F.13 was found in a torpedo-shaped iron coffin and had a proposed burial date of 1861 based on the nameplate, identifying that it contained Mary B. Rhem, whose reported dates of birth and death are 1860-1861 (Stewart, 2022). The coffin was located on the south shelves of the family vault (Stewart, 2022). Along with the remains, the interior of the coffin contained an intact coffin lining around the viewing window and bottom portion of the coffin. Additionally, a dress or burial shroud was intact (Stewart, 2022). The majority of the bones were

covered in a dried, powdery tissue, and the bones themselves were of a papier-mâché-like consistency, as if there was no mineral component left in the bones. This made it difficult to remove the tissue without destroying the bone while conducting observations. No metallic staining or rusted coloration was noted.



Figure 19: Individual F.13 skeletal remains. Remains were unable to be identified for skeletal inventory and pathological analysis. Photograph taken by Dr. Megan Perry.



Figure 20a: Vertebral bodies (16) recovered from F.13. Photograph taken by Dr. Megan Perry.



Figure 20b: Skulls, upper limbs, and ribs of F.13. Photograph taken by Dr. Megan Perry.



Figure 21: Coffin F.13 and contents. Note coloration of skull (right) and textile preservation throughout. Photograph taken by Jalyann Stewart.

The feet of this individual were held in chunks of soft tissue and only recognizable by their shape. Most of the lower part of the body could not be identified or associated with a particular body part. Sixteen vertebral bodies (Figure 20a) and approximately ten pieces of the neural arch were preserved along with a cranium, upper limbs, and ribs (Figure 20b). The vertebral bodies and neural arches were light in color and friable, crumbling easily during examination. The cranium, upper limbs, and ribs were much darker in color and much less fragile. Dental age estimation indicated that this individual 7.5 months  $\pm$  3 months of age close to Mary B. Rhem's reported age of death of 1 year.

#### F.19

Individual F.19 was recovered from a torpedo-shaped iron coffin located on the south shelves of the vault. The coffin included a name plate identifying the individual as Hugh Dudley

Rhem, whose reported dates of birth and death were 1872-1873 (Stewart, 2022). Bone and coffin material were scattered throughout the coffin, and the coffin and remains were poorly preserved. The bones were brittle and crumbled easily despite careful handling, and very few bones were complete. Six right thoracic vertebrae neural arches were still articulated by soft tissue.



Figure 22: Individual F.19 photographed for skeletal inventory. Photograph taken by Dr. Megan Perry.



Figure 23: Coffin F.19 and contents. Photograph taken by Jalyynn Stewart.

A dark rusted color was present throughout the skeleton with some areas having a metallic shine. The skull specifically showed a clear distinction between areas that did not present this coloration and those that did. In terms of weathering, the femurs showed flaking typical of water damage. The age of F.19 was estimated to be birth  $\pm$  2 weeks based on dental formation and bone metrics. However, this contrasted with the reported age at death provided by Rhem Family documents, which was 1 year (Joseph L. Rhem Family Bible, 1860/2020).

#### *XRF Analysis*

A total of three to four samples of each individual was tested using pXRF analysis. Each set of samples included bone and soft tissue remains as well as areas of metallic staining when applicable. Coffins F.02, F.06, and F.07 were also analyzed using pXRF. For each individual,

one spectrum was produced that included all of the tested samples, and an additional spectrum that included the coffin scan was produced for F.02, F.06, and F.07.

For F.01, the pelvic ilium (F.01.1), lower leg and foot encased in mummified soft tissue (F.01.2), and occipital bone were examined (F.01.3).

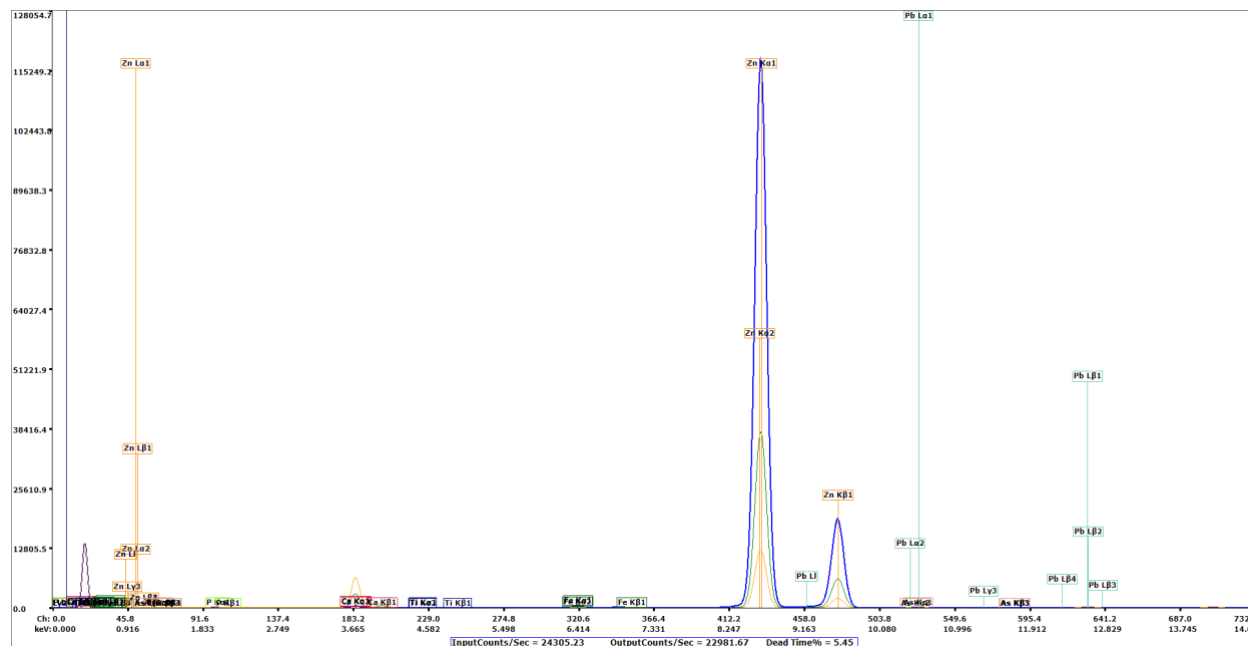


Figure 24: pXRF spectrum of the human remains from F.01. The samples tested included the pelvic ilium (F.01.1, red), lower leg and foot (F.01.2, blue), and occipital bone (F.01.3, green).

Along with the elements typically found in human bone, high levels of zinc (Zn) were found, and only traces of iron (Fe), tin (Ti), and lead (Pb) were detected. This indicated that the coffin itself was made of zinc instead of iron.

For F.02, the temporal bone (F.02.1), femur (F.02.2), maxilla bone (F.02.3), and scapula (F.02.4) were examined. Additionally, the coffin of this individual was examined (F.02.5).

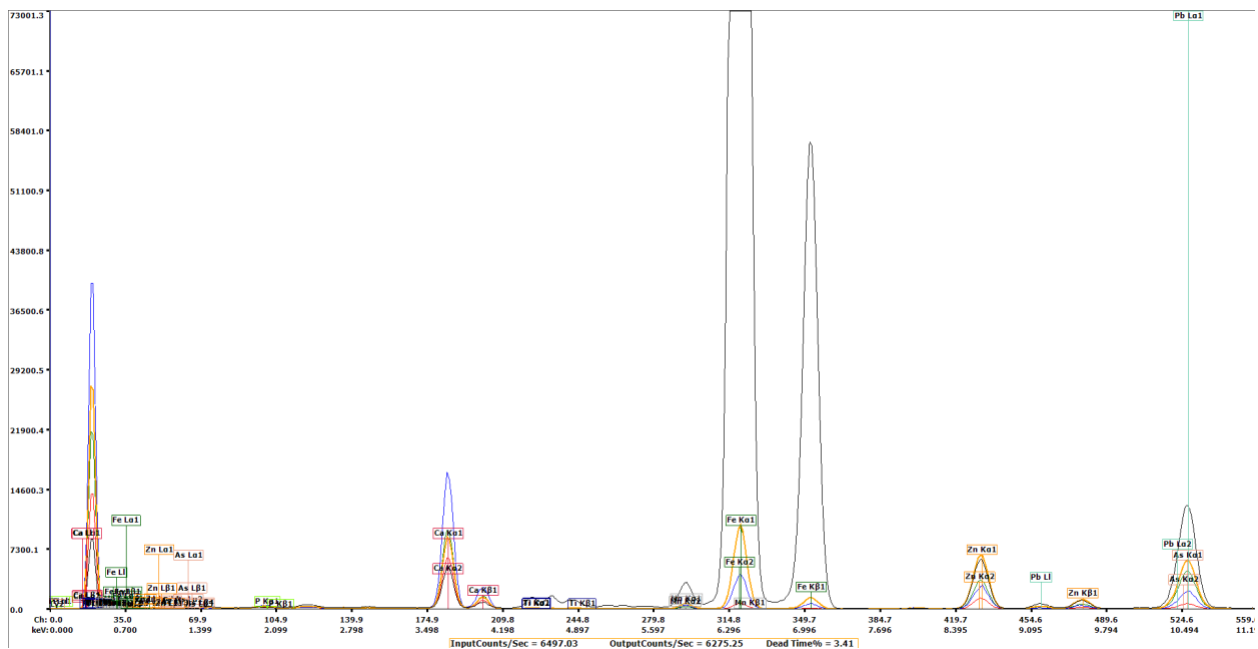


Figure 25: pXRF spectrum of F.01 human remains and coffin. The samples tested included the temporal bone (F.02.1, red), femur (F.02.2, blue), maxilla bone (F.02.3, green), scapula (F.02.4, orange), and coffin (F.02.5, black).

F.02 samples had even higher peaks of elements known to be found in human bone.

Additionally, high levels of iron (Fe) and lead (Pb) were detected, indicating the make-up of the coffin. Zinc (Zn) and tin (Ti) were also detected. The F.02 spectrum is also a good example of how difficult it can be to identify the presence of arsenic when there are high levels of lead within a sample (Figure 26). This is a known issue with pXRF, due to the closeness of the arsenic (As) peak to the lead (Pb) peak (Figure 26) (EPA, N.d.)

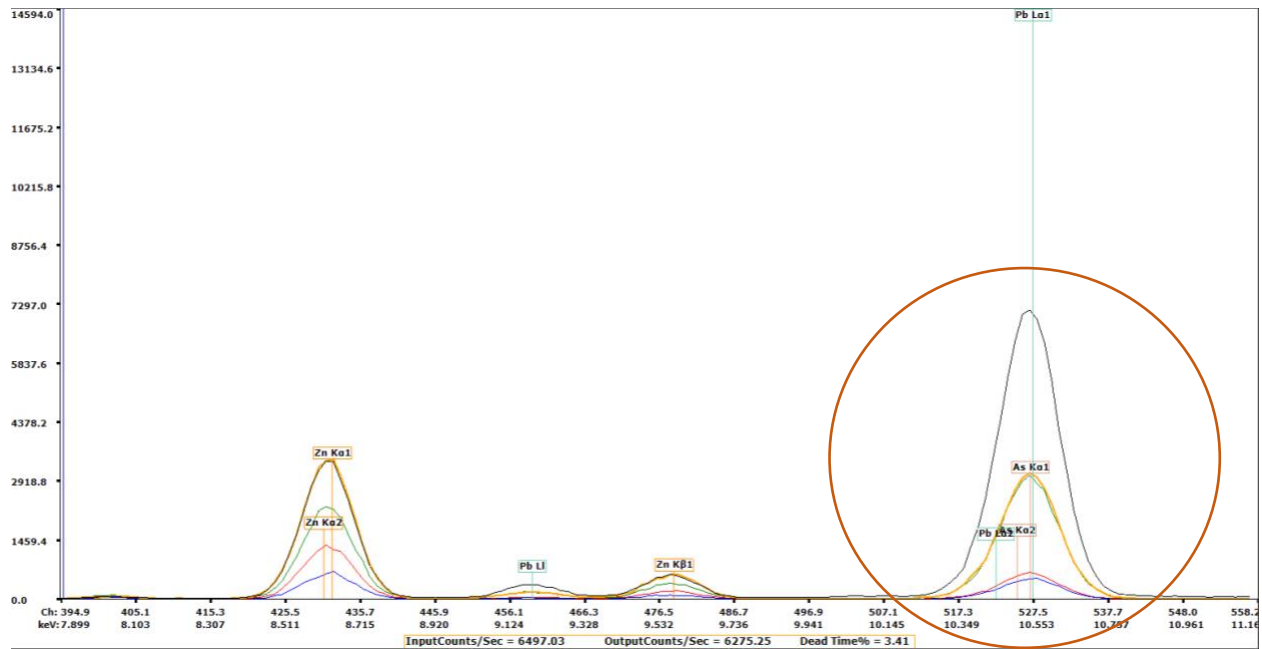


Figure 26: Arsenic (As) and Lead (Pb) pXRF peaks. Note how close the peaks are to each other. Image obtained from F.02 human remains pXRF spectrum.

For F.06, the occipital bone (F.06.1), femur (F.06.2), and right portion of the frontal bone (F.06.3) were examined. Additionally, the coffin of this individual was examined (F.06.4).

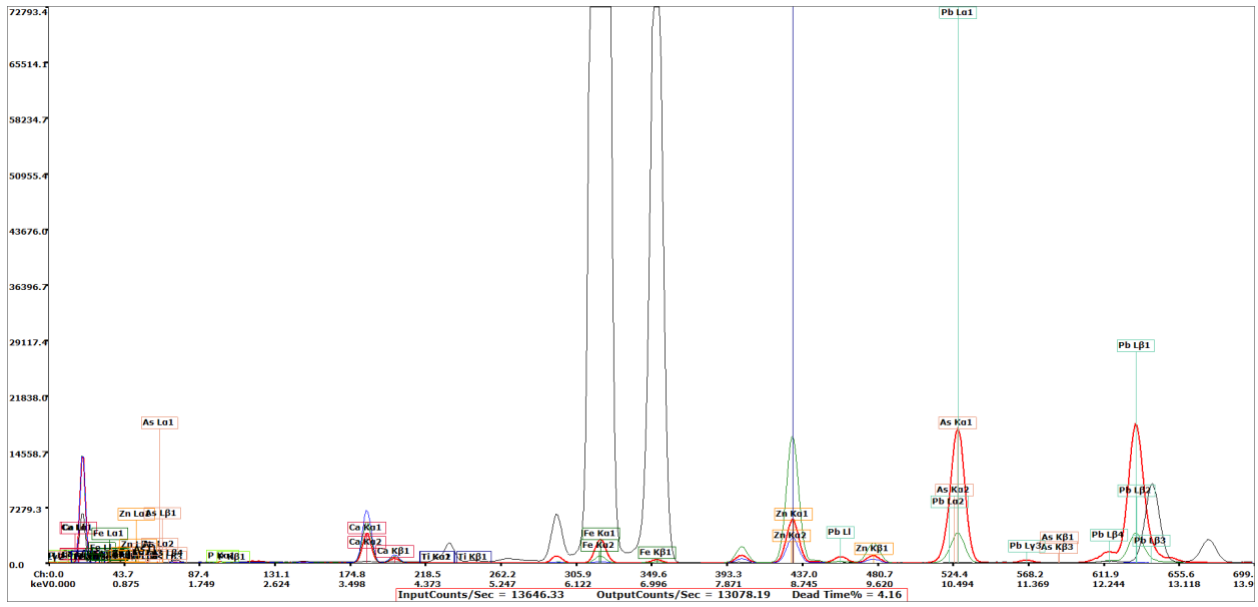


Figure 27: pXRF spectrum of F.06 human remains and coffin. The samples tested included the occipital bone (F.06.1, red), femur (F.06.2, blue), frontal bone (F.06.3, green), and coffin (F.06.4, black).

The spectrum produced from F.06 testing revealed that the coffin was mainly made of iron (Fe) and likely sealed by lead (Pb). Traces of zinc (Zn) and tin (Ti) were also observed. Elements typical of bone composition were detected as well.

For F.07, the lower arm encased in soft tissue (F.07.1), femur (F.07.2), and a sample of just soft tissue (F.07.3) were examined. Additionally, the coffin of this individual was examined (F.07.4).

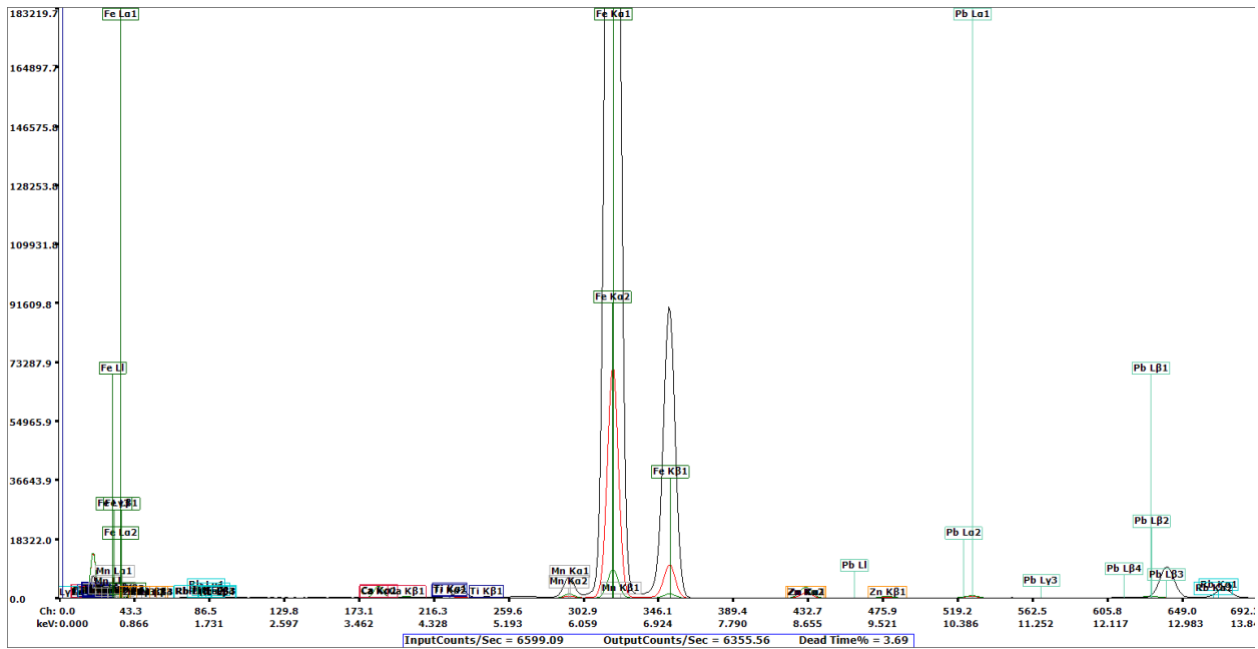


Figure 28: pXRF spectrum of F.07 human remains and coffin. The samples tested included the lower arm and soft tissue (F.07.1, red), femur (F.07.2, blue), soft tissue (F.07.3, green), and coffin (F.07.4, black).

F.07 contained high levels of iron (Fe) and lead (Pb) as well as smaller traces of zinc (Zn), tin (Ti), and manganese (Mn). Traces of elements found in human bone can also be seen.

For F.08, a sample of just soft tissue (F.08.1), the scapula (F.08.2), right portion of the ribcage and soft tissue (F.08.3), and an unknown material (F.08.4) found throughout the coffin were examined.

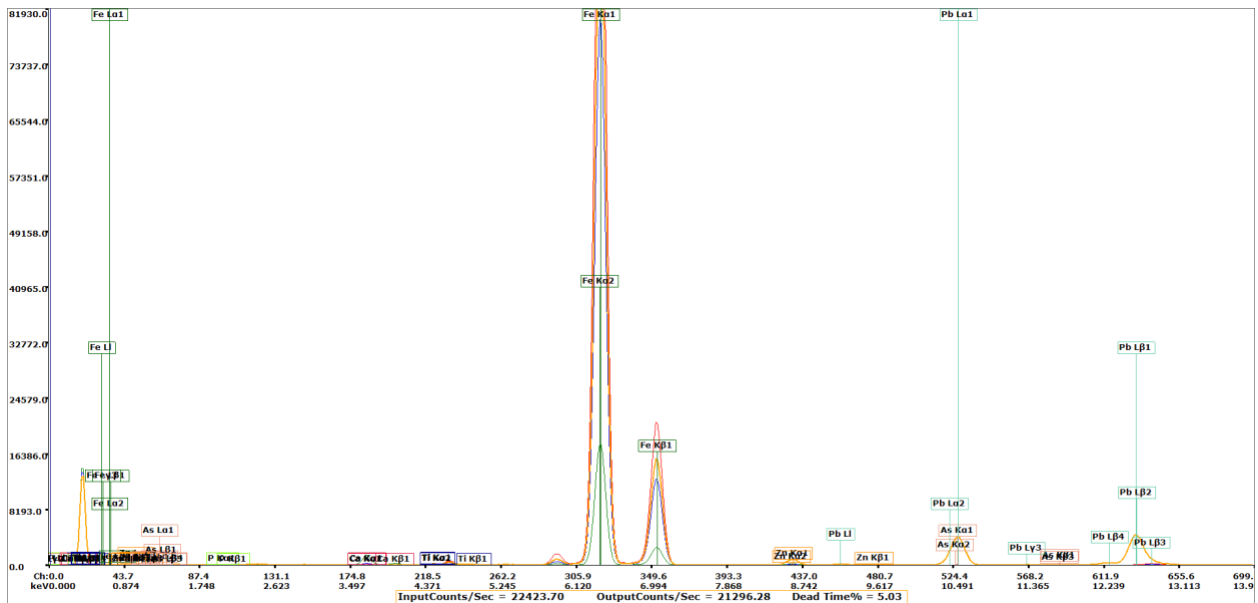


Figure 29: pXRF spectrum of F.08 human remains. The samples tested included soft tissue (F.08.1, red), the scapula (F.08.2, blue), a portion of the ribcage and soft tissue (F.08.3, green), and an unknown material (F.08.4, orange).

XRF analysis of F.08 revealed very high levels of iron (Fe). Traces of zinc (Zn), tin (Ti), and lead (Pb) are also shown on the spectrum, as well as elements expected to be seen in human bone. The unknown material (F.08.4), shown in orange, had particularly high peaks of iron (Fe) and lead (Pb).

For F.12, a pelvic ilium (F.12.1), femur (F.12.2), and the right foot encased in soft tissue (F.12.3) were examined.

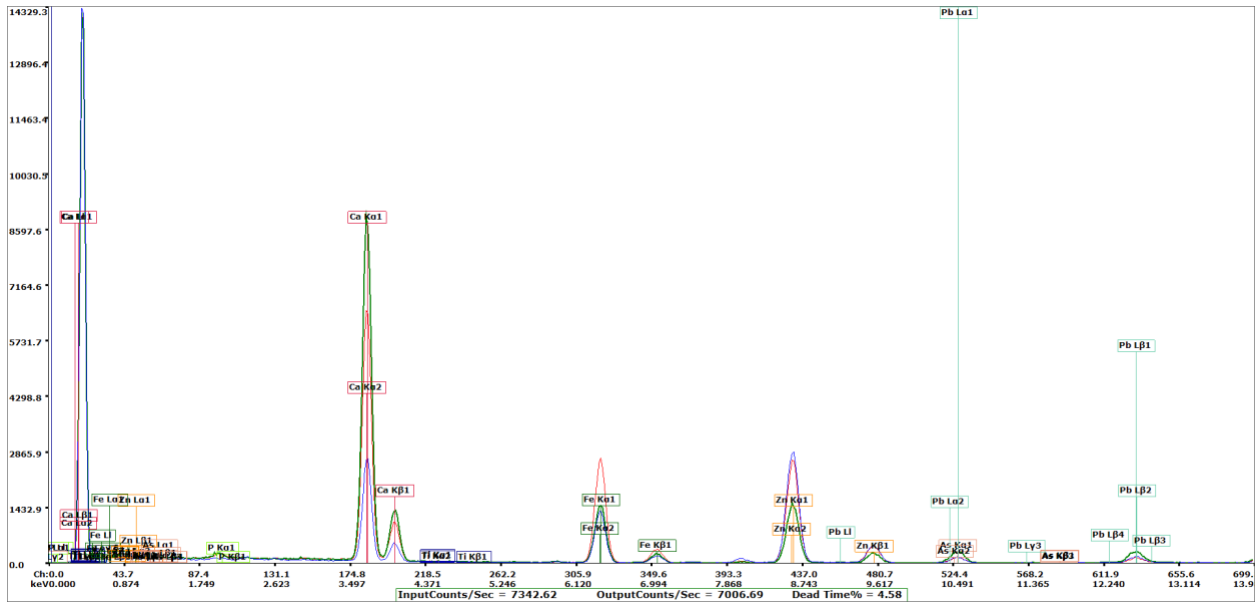


Figure 30: pXRF spectrum of F.12 human remains. The samples tested included a pelvic ilium (F.12.1, red), femur (F.12.2, blue), and the right foot and soft tissue (F.12.3, green).

F.12 pXRF analysis revealed much higher levels of elements typical of human bone composition, such as calcium (Ca) and potassium (K). There were also peaks indicating the presence of iron (Fe), zinc (Zn), lead (Pb), and tin (Ti), but they were much lower than that of previously tested samples.

For F.13, the fibula (F.13.1), a cranial bone (F.13.2), and an ilium (F.12.3) were examined.

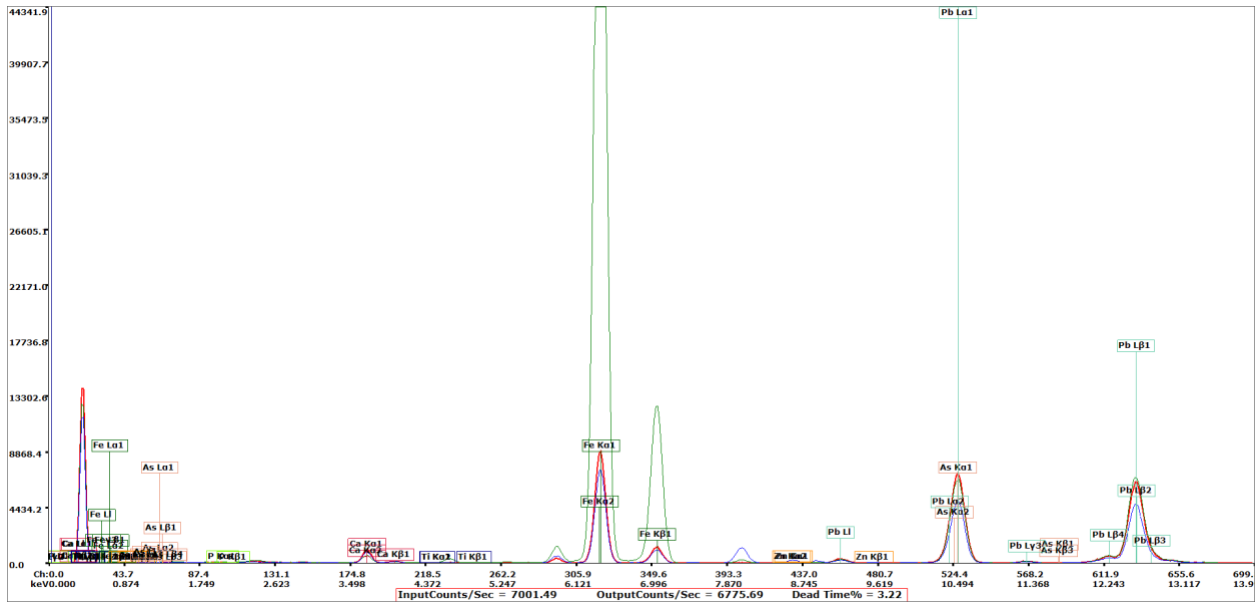


Figure 31: pXRF spectrum of F.13 human remains. The samples tested included a fibula (F.13.1, red), cranial bone (F.13.2, blue), and ilium (F.13.3, green).

F.13 analysis shows high levels of iron (Fe) along with zinc (Zn), tin (Ti), and lead (Pb).

For F.19, a cranial bone (F.19.1), tibia (F.19.2), frontal bone (F.19.3), and vertebrae held in soft tissue (F.19.4) were examined.

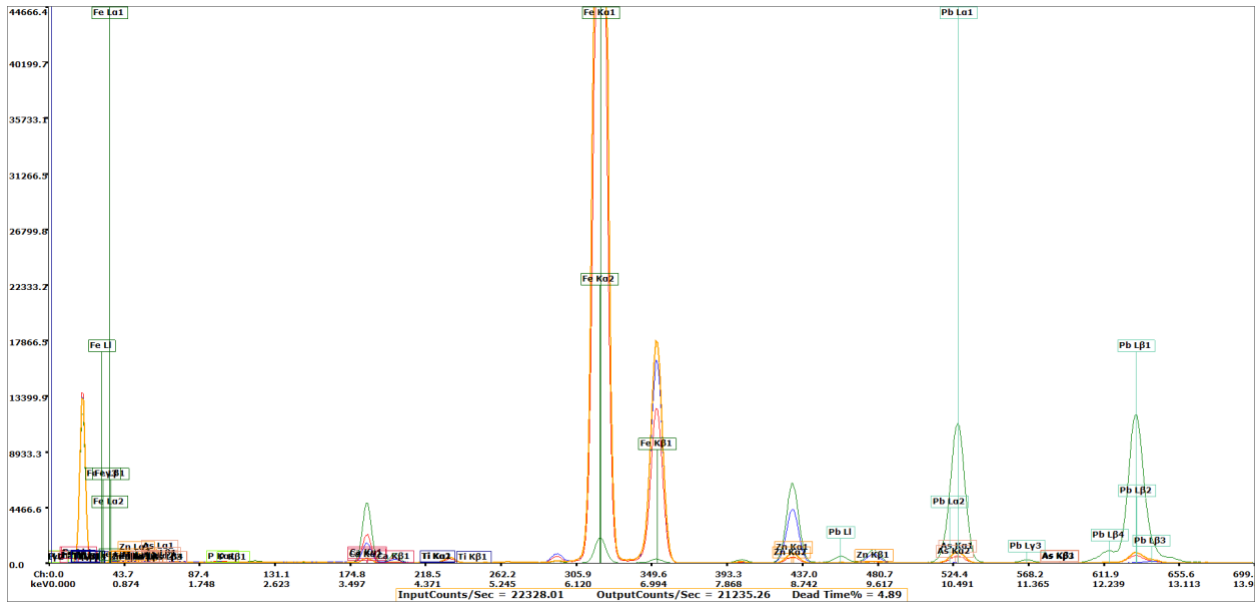


Figure 32: pXRF spectrum of F.19 human remains. The samples tested included a cranial bone (F.19.1, red), tibia (F.19.2, blue), frontal bone (F.19.3, green), and vertebrae with soft tissue (F.19.4, orange).

F.19 contained very high levels of iron (Fe), lead (Pb), and zinc (Zn). Additionally, traces of tin (Ti) were found, as well as elements typical of human bone composition.

## Discussion

Results show a direct correlation between the preservation of human remains and the condition of the burial environment. In general, individuals found in coffins that were intact or only slightly damaged were more complete, showed minimal signs of weathering, and had greater preservation of bones, soft tissue, and clothing. In contrast, individuals recovered from damaged coffins were generally less complete, were more weathered, and had little to no soft tissue or textile preservation. These findings were similar to those of Owsley and Compton (1997) who note that excellent preservation of bones, soft tissue, and artifacts, such as clothing and personal items, is typical of iron coffin environments. Bricker et al. (2013) also reports fair skeletal preservations but only noted clothing preservation in one of the six burials studied. The

study found that all skeletal remains from iron coffins exhibited exfoliation, demineralization, and a color range of dark orange to black on outer bone cortices (Bricker et al., 2013). Pokines and Baker (2013) suggest that the anaerobic environment created by the iron coffin may be like that of wet, iron-pan soil burial mounds, which allows for excellent long-term preservation of organic materials (Breuning-Madsen et al., 2001). Owsley et al. (2006) found iron coffin remains, dated to be from the mid-19<sup>th</sup> century to early 20<sup>th</sup> century, to be well-preserved, darkly stained, and fully clothed. Testing for embalming chemicals was also negative (Owsley et al., 2006). This, along with the overall preservation trends found by both Owsley et al. (2006) and Bricker et al. (2013) was generally what was found in this study. However, no soft tissue preservation was reported by either Owsley et al. (2006) or Bricker et al. (2013). Additionally, the presence of textiles played a role in the preservation of the skeletal remains in that the clothing was usually better preserved than the skeletal elements within it (Lipkin, 2021). This does not necessarily mean that the individuals wrapped in a textile were more or less preserved, but that the overall preservation of said individuals was less uniform or consistent throughout the body than of those that were not found wrapped in a textile.

The rusted coloration of many of the individuals was unusual and thus of significant interest in this investigation. According to both Owsley and Compton (1997) and Shultz et al. (2003), it is common for human remains in iron coffins to be stained dark as a result of mineral oxide leaching that occurs after the coffin is breached and decomposition processes begin. However, iron oxide, or rust, staining is not common (Pokines and Baker, 2013).

Portable XRF analysis demonstrated that all except one (F.01) of the eight coffins examined were mainly made of iron. The pXRF analysis revealed that leaching of the coffin materials, primarily lead and iron, was the cause of discoloration of bone and soft tissue remains.

While only three of the coffin interiors and exteriors were analyzed using pXRF (F.02, F.06, and F.07), the pXRF spectra of the samples of human remains show significant peaks for iron (Fe) and lead (Pb). Because these elements are not naturally found in human remains (Brenner, 2014), the claim can be made that their presence is due to a chemical reaction that occurred within the coffin environment. Bricker et al. (2013) reports the bone chemistry of iron coffin remains indicating the process of iron sulfurization as a result of the acidity of the acid sulfates present in the iron coffins as well as the combination of natural decomposition and lead sulfate from the interior paint of the coffin. Like that of overall preservation and coffin condition, the correlation between metallic staining and coffin condition is strong, such that coffins that remained intact, such as F.07, held remains which had more prevalent and more intense cases of metallic staining. Individuals that were recovered from damaged coffins, such as F.02, had smaller peaks of iron and lead. However, traces of iron and lead were still detected in these individuals, indicating that even damaged, the metallic coffin environment has an effect on the remains within it. Individual F.01 was interred within a coffin made primarily of zinc (Zn), as indicated by the pXRF spectrum (Figure 24) which also had an impact on the state of the remains. Moreover, analysis using pXRF revealed that samples containing soft tissue held higher traces of coffin materials than samples that were just bone. It can therefore be concluded that the metallic coffin environment has a more significant effect on soft tissue remains than bone in terms of elemental composition.

Finally, pXRF analysis provided no clear evidence of embalming with arsenic or other embalming chemicals. It can be assumed that these children most likely died close to home and were buried quickly and, therefore, embalming was not necessary. This is not to say that the

Rhem Family was not concerned with the preservation of these individuals. Their use of these expensive iron coffins speaks to both their high social status and respect for the dead.

## **Conclusion**

The main goals of this thesis were to complete a full analysis of the preservation of the subadult individuals interred in metallic coffins in the Rhem Family Vault and to determine the effects of the metallic coffin environments on the remains. This was to better understand the taphonomic trends caused by metal coffins and the varying results found across different studies. The subjects of this study included eight subadult individuals interred in metallic coffins inside the family vault during the mid-nineteenth century. Information of the state of each coffin and preliminary observations of their contents were gathered from previous research on the Rhem Family Vault (Stewart, 2022). A full inventory, taphonomic analysis, pathological analysis, age estimation, and pXRF analysis was completed. It was concluded that the bone taphonomy differed based on whether the coffin remained intact and sealed and on the presence of textiles around the bones, that the pXRF analysis demonstrated that the human skeletal remains in the coffins were impacted by the metals used in their burial container, and that no clear evidence of embalming with chemicals typical of embalming methods of the time period was found. Based on pXRF analysis, it can also be concluded that all of the coffins examined were mainly made of iron and sealed with lead with the exception of one (F.01) which was made mostly of zinc.

## *Future Research*

Throughout this investigation and previous research conducted by Stewart (2022), several samples from the individuals were collected. Hair and nail samples that had been well preserved

in some cases could likely be used for DNA testing. This kind of research can help to potentially identify more of the individuals and confirm their relationship to the Rhem Family ancestors. Additionally, the diet and mobility of the Rhem Family can be investigated via isotope testing. This may provide more understanding of the state of the remains excavated from the vault as well as supply insight into the lifestyle of the Rhem family members during this time period. Investigation of the clothing and textile samples preserved could allow for further knowledge of social status, financial status, and mortuary behaviors of this time period, specifically where children are concerned. Comparing the findings of this study with the decomposition states of other Rhem family members interred in the vault would help to provide a good comparison to the effects of iron coffins on human remains to that of other burial containers. Lastly, conducting additional research on subadult remains buried in iron coffins in other cases would produce a broader understanding of the results found here.

## References

Adan-Bayewitz, D., F. Asaro, and R. D. GIAUQUE.

1999 Determining pottery provenance: Application of a new high-precision X-ray fluorescence method and comparison with instrumental neutron activation analysis. *Archaeometry*, 41(1), 1-24.

Allen IV, D. S.

2002 The mason coffins: Metallic burial cases in the central south. In *4th South Central Historical Archaeology Conference, Jackson, MS*.

AlQahtani S. J., H. M. Liversidge, and M. P. Hector

2010 Atlas of tooth development and eruption. *American Journal of Physical Anthropology* 142(3):481-90.

Andrade E., C. Solís, C. E. Canto, O. G. De Lucio, E. Chavez, M. F. Rocha, O. Villanueva, and C. A. Torreblanca

2014 Radiocarbon dating and compositional analysis of pre-Columbian human bones. *Nuclear Instruments and Methods in Physics Research, B* 332:303-307.

Beckhoff, B., B. Kanngießler, N. Langhoff, R. Wendell, and H. Wolff, editors

2007 *Handbook of Practical X-ray Fluorescence Analysis*. Springer Science & Business Media.

Berryman, H. E., W. M. Bass, S. A. Symes, and O. B. Smith

1991 Recognition of cemetery remains in the forensic setting. *Journal of Forensic Sciences*, 36(1), 230-237.

Behrensmeyer, A. K.

1978 Taphonomic and ecologic information from bone weathering. *Paleobiology*, 4(2), 150-162.

Berkowitz, E.

2006 *X-Ray physics*. MIT Department of Physics.

Brenner, E.

2014 Human body preservation—old and new techniques. *Journal of anatomy*, 224(3), 316-344.

Bricker, C. M., D. W. Owsley, K. S. Bruwelheide, and D. A. Hull-Walski

2013 Identification and taphonomic analysis of iron coffin burials from southeast Virginia.

Brouwer, P.

2006 Theory of XRF. *Almelo, Netherlands: PANalytical BV*.

Buikstra J. E., and D. H. Ubelaker

1994 *Standards for Data Collection from Human Skeletal Remains*. Fayetteville: Arkansas Archaeological Survey.

Blumenthal, N. C.

1990 The in vitro uptake of trace elements by hydroxyapatite. *Trace metals and fluoride in bones and teeth*. Boca Raton: CRC Press, 307-314.

Breuning-Madsen, H., M. K. Holst, and M. Rasmussen

2001 The chemical environment in a burial mound shortly after construction – an archaeological pedological experiment. *Journal of Archaeological Science*, 28(7), 691-697.

Cardoso, H. F. V., J. Abrantes, L. T. Humphrey

2014 Age estimation of immature human skeletal remains from the diaphyseal length of the long bones in the postnatal period. *International Journal of Legal Medicine*, 128, 809-824.

Cardoso H. F., L. Spake, L. T. Humphrey

2017 Age estimation of immature human skeletal remains from the dimensions of the girdle bones in the postnatal period. *American Journal of Physical Anthropology*, 163(4), 772-783.

Carvalho, M. L., A. F. Marques, M. T. Lima, and U. Reus

2004 Trace elements distribution and post-mortem intake in human bones from Middle Age by total reflection X-ray fluorescence. *Spectrochimica Acta Part B: Atomic Spectroscopy*, 59(8), 1251-1257.

Çirak, M.T.

2016 Anthropological assessment of element levels in anemic individuals. *Turk. Stud.*, 12, 169-178.

Conrey, R. M., M. Goodman-Elgar, N. Bettencourt, A. Seyfarth, A. Van Hoose, and J. A. Wolff

2014 Calibration of a portable X-ray fluorescence spectrometer in the analysis of archaeological samples using influence coefficients. *Geochemistry: Exploration, Environment, Analysis*, 14(3), 291-301.

Cone, B.

2013 *Bioarchaeology of Urban Versus Rural Historic North Carolina Family Cemeteries*. East Carolina University.

Cundiff, F. B. Clark, and K. Miller

2021. Portable X-Ray fluorescence (pXRF) analysis of Egyptian mortuary practices: A case study. In: Koons, M., MacLeod, C. (Eds.), *The Egyptian Mummies and Coffins of the Denver Museum of Nature & Science: History, Technical Analysis, and Conservation*. University Press of Colorado, Denver, pp. 111-138.

Cunningham, C., L. Scheuer, and S. Black

2016 *Developmental juvenile osteology*. Academic press.

Dupras, T. L., and J. J. Schultz

2013 Taphonomic bone staining and color changes in forensic contexts. *Manual of forensic taphonomy*, 315-340.

Environmental Protection Agency

N.D. Lead-arsenic interferences with XRF. Report on file, EPA Region 5 Records Center, number 259870 Retrieved April 18, 2024, from <https://semspub.epa.gov/work/05/259870.pdf>.

Ezugworie, J., C. Anibeze, F. Ozoemena, J. Ezugworie, and C. Anibeze

2009 Trends in the development of embalming methods. *Internet J Altern Med* 7.

Fazekas, I. G., and F. Kósa

1978 *Forensic fetal osteology*. Budapest: Akadémiai Kiadó.

Fernandes, R., B. J. van Os, and H. D. Huisman

2013 The use of Hand-Held XRF for investigating the composition and corrosion of Roman copper-alloyed artifacts. *Heritage Science*, 1, 1-7.

Geddes, G. E.

1981 *Welcome Joy: Death in Puritan New England*. UMI Research Press: Ann Arbor, Michigan.

Granite, G. E.

2012 *Portable X-ray fluorescence spectroscopy and its research applications to Northern European bog bodies*. State University of New York at Buffalo.

Gomes, R. A., L. Catarino, and A. L. Santos

2021 Anemia, cribra cranii and elemental composition using portable X-ray fluorescence: A study in individuals from the Coimbra Identified Osteological Collections. *Journal of Archaeological Science*, 136, 105514.

Gomes, R. A., A. L. Santos, and L. Catarino

2024 Elemental analysis using portable X-ray fluorescence: Guidelines for the study of dry human bone. *International Journal of Paleopathology*, 44, 85-89.

Haglund, W. D. and Sorg, M. H. (Eds.)

2001 *Advances in Forensic Taphonomy*. CRC Press.

Hand, B.

2021 *Dem bones : Cedar Grove crypt is cleaned out to make way for renovations*. New Bern Live: New Bern, North Carolina.

Henderson, C. Y., G. A. King, A. C. Caffell, and R. Allen

2015 Adipocere inside nineteenth century femora: The effect of grave conditions. *International Journal of Osteoarchaeology*, 25(6), 960-967.

Ioannou, S., D. Hunt, and M. Henneberg

2017 Five cases of dental anomalies attributable to congenital syphilis from early 20th century American anatomical collections. *Dental Anthropology Journal*, 30(1), 25-37.

Iqbal, M. A., M. Ueland, and S. L. Forbes

2020 Recent advances in the estimation of post-mortem interval in forensic taphonomy. *Australian Journal of Forensic Sciences*, 52(1), 107–123.

Joseph L. Rhem Family Bible

*The Holy Bible* (William M. Harding, Philadelphia 1860); original owned in 2020 by Deborah A. Cordes Porcelli and David A. French passed down from Joseph L. Rhem.

Kilburn, N. N., R. L. Gowland, H. H. Halldórsdóttir, R. Williams, and T. J. Thompson

2021 Assessing pathological conditions in archaeological bone using portable X-ray fluorescence (pXRF). *Journal of Archaeological Science: Reports*, 37, 102980.

Knüsel, C. J., and J. Robb

2016 Funerary taphonomy: An overview of goals and methods. *Journal of Archaeological Science: Reports*, 10, 655-673.

LeeDecker C. H.

2009 Preparing for an Afterlife on Earth: The Transformation of Mortuary Behavior in Nineteenth-Century North America. In *International Handbook of Historical Archaeology* (pp. 141-157). New York, NY: Springer New York.

Lipkin, S., E. Ruhl, K. Vajanto, A. Tranberg, and J. Suomela

2021 Textiles: Decay and preservation in seventeenth-to nineteenth-century burials in Finland. *Historical Archaeology*, 55, 49-64.

López-Costas, O., O. Lantes-Suarez, and A. M. Cortizas

2016 Chemical compositional changes in archaeological human bones due to diagenesis:

Type of bone vs soil environment. *Journal of archaeological Science*, 67, 43-51.

Magalhaes, B. M., L. Catarino, I. Carreiro, R. A. Gomes, R. R. Gaspar, V. M. Matos., and A. L. Santos

2021 Differential diagnosis of a diffuse sclerosis in an identified male skull (early 20th century Coimbra, Portugal): A multimethodological approach for the identification of osteosclerotic dysplasias in skeletonized individuals. *International Journal of Paleopathology*, 34, 134-141.

McGarry, A., B. Floyd, and J. Littleton

2021 Using portable X-ray fluorescence (pXRF) spectrometry to discriminate burned skeletal fragments. *Archaeological and Anthropological Sciences*, 13(7), 117.

Miller, H. M., S. D. Hurry, and T. B. Riordan

2004 The lead coffins of St. Mary's City: An exploration of life and death in early Maryland. *Maryland Historical Magazine*, 99(3), 351-373.

Murphy, L., B. G. Barnett, R. G. Holloway, and C. M. Sheldon

1981 An experiment to determine the effects of wet/dry cycling on certain common cultural materials. *The final report of the National Reservoir Inundation Study. Technical Report*, 8-1.

Nganvongpanit, K., K. Buddhachat, S. Klinhom, P. Kaewmong, C. Thitaram, and P.

Mahakkanukrauh

2016 Determining comparative elemental profile using handheld X-ray fluorescence in humans, elephants, dogs, and dolphins: Preliminary study for species identification. *Forensic science international*, 263, 101–106.

Owsley, D. W., and B. E. Compton

1997 Preservation in late 19th Century iron coffin burials. In *Forensic Taphonomy: The Postmortem Fate of Human Remains* (pp. 511-526). CRC Press

Owsley, D. W., K. S. Bruwelheide, L. W. Cartmell, L. E. Burgess, S. J. Foote, S. M. Chang, and N. Fielder

2006 The man in the iron coffin: An interdisciplinary effort to name the past. *Historical Archaeology*, 40, 89-108.

Pemmer, B., A. Roschger, A. Wastl, J. G. Hofstaetter, P. Wobrauschek, R. Simon, H. W. Thaler, P. Rschger, K. Klaushofer, and C. Streli

2013 Spatial distribution of the trace elements zinc, strontium and lead in human bone tissue. *Bone*, 57(1), 184-193.

Perrone, A., J. E. Finlayson, E. J. Bartelink, and K. D. Dalton

2014 Application of portable X-ray fluorescence (XRF) for sorting commingled human remains. In *Commingled human remains* (pp. 145-165). Academic Press.

Pokines, J. T.

2015 Forensic recoveries of U.S. war dead and the effects of taphonomy and other site altering processes. In *Hard evidence:* (pp. 141-154). Routledge.

Pokines, J.T., and J. E. Baker

2013 Effects of Burial Environment on Osseous Remains. In *Manual of Forensic Taphonomy* (pp. 103-162). CRC Press.

Pokines, J. T., K. Faillace, J. Berger, D. Pirtle, M. Sharpe, A. Curtis, K. Lombardi, and J. Admans

2018 The effects of repeated wet-dry cycles as a component of bone weathering. *Journal of Archaeological Science: Reports*, 17, 433-441.

Pokines, J.T., D. P. Zinni, and K. Crowley

2016 Taphonomic patterning of cemetery remains received at the office of the chief medical examiner, Boston, Massachusetts. *Journal of Forensic Sciences*, 61, S71-S81.

Quintana, J. R.

2019 *As the Sun Sets, We Remain: A Bioarchaeological Analysis of the Gause Cemetery at Seaside*. East Carolina University.

Rainville, L.

1999 Hanover deathscapes: Mortuary variability in New Hampshire, 1770-1920. *Ethnohistory*, 541-597.

Rogers, T. L.

2005 Recognition of cemetery remains in a forensic context. *Journal of Forensic Sciences*, 50(1), JFS2003398-7.

Santos, A. L.

2020 A particular heritage: The importance of identified osteological collections. *Mètode Science Studies Journal*, 10, 91-97.

Scheuer, L., and S. Black

2000 Development and ageing of the juvenile skeleton. *Human Osteology in Archaeology and Forensic Science*, 9-22.

Schultz J. J., M. Williamson, S. P. Nawrocki, A. Falsetti, M. Warren

2003 A taphonomic profile to aid in the recognition of human remains from historic and/or cemetery contexts. *Florida Anthropologist*, 56(2), 141-147.

Scientific, T. F.

2020 What is XRF (X-ray fluorescence) and how does it work. *ThermoFisher Scientific Ask a Scientist*.

Sledzik P. S., and M. S. Micozzi

19978 Autopsied, embalmed, and preserved human remains: distinguishing features in forensic and historic contexts. In *Forensic taphonomy: the postmortem fate of human remains* (pp. 483-495). CRC Press.

Sorg, M. H., and W. D. Haglund (Eds.).

1996 *Forensic taphonomy: the postmortem fate of human remains*. CRC Press.

Specht, A. J., A. S. Dickerson, and M. G. Weisskopf

2019 Comparison of bone lead measured via portable x-ray fluorescence across and within bones. *Environmental research*, 172, 273–278.

Specht, A. J., F. Mostafaei, Y. Lin, J. Xu, and L. H. Nie

2017 Measurements of strontium levels in human bone in vivo using portable X-ray fluorescence (XRF). *Applied spectroscopy*, 71(8), 1962-1968.

Specht, A. J., M. Weisskopf, and L. H. Nie

2014 Portable XRF Technology to Quantify Pb in Bone In Vivo. *Journal of Biomarkers*, 2014.

Stewart, J. E.

2022 *Mortuary Archaeology of a 19<sup>th</sup>-20<sup>th</sup> Century Family Tomb in New Bern, North Carolina* (Master's Thesis East Carolina University).

Woodard, H. Q.

1962 The elementary composition of human cortical bone. *Health Physics*, 8(5), 513-517.

Zdral, S., Á. M. Monge Calleja, L. Catarino, F. Curate, and A. L. Santos

2021 Elemental composition in female dry femora using portable X-ray fluorescence (pXRF): Association with age and osteoporosis. *Calcified Tissue International*, 109, 231-240.

Zhou, S., Q. Cheng, D. C. Weindorf, B. Yang, Z. Yuan, and J. Yang

2022 Determination of trace element concentrations in organic materials of “intermediate-thickness” via portable X-ray fluorescence spectrometry. *Journal of Analytical Atomic Spectrometry*, 37(11), 2461-2469.

Zimmerman, H. A., C. J. Meizel-Lambert, J. J. Schultz, and M. E. Sigman

2015 Chemical differentiation of osseous, dental, and non-skeletal materials in forensic anthropology using elemental analysis. *Science & Justice*, 55(2), 131–138.

Zuckerman, M.

2016 More harm than healing? Investigating the iatrogenic effects of mercury treatment on acquired syphilis in post-medieval London. *Open Archaeology*, 2(1).